materials

MDPI

Article

Preparation of Cotton–Zinc Composites by Magnetron Sputtering Metallization and Evaluation of their Antimicrobial Properties and Cytotoxicity

Marcin Henryk Kudzin [1,*], Małgorzata Giełdowska [1], Paulina Król [1] and Zuzanna Sobańska [2]

[1] Łukasiewicz Research Network—Łódz Institute of Technology, 19/27 Marii Sklodowskiej-Curie Str., 90-570 Łódz, Poland; malgorzata.gieldowska@lit.lukasiewicz.gov.pl (M.G.); paulina.krol@lit.lukasiewicz.gov.pl (P.K.)

[2] Nofer Institute of Occupational Medicine, Św. Teresy od Dzieciątka Jezus 8, 91-348 Łódz, Poland; zuzanna.sobanska@imp.lodz.pl

* Correspondence: marcin.kudzin@lit.lukasiewicz.gov.pl; Tel.: +48-42-6163121

Abstract: The aim of this investigation was to evaluate the biological properties of cotton–zinc composites. A coating of zinc (Zn) on a cotton fabric was successfully obtained by a DC magnetron sputtering system using a metallic Zn target (99.9%). The new composite was characterized using scanning electron microscopy/energy-dispersive X-ray spectroscopy (SEM/EDS), UV/Vis transmittance, and atomic absorption spectrometry with flame excitation (FAAS). The composite was tested for microbial activity against colonies of Gram-positive (*Staphylococcus aureus*) and Gram-negative (*Escherichia coli*) bacteria and antifungal activity against *Aspergillus niger* and *Chaetomium globosum* fungal mold species as model microorganisms. Cytotoxicity screening of the tested modified material was carried out on BALB/3T3 clone mouse fibroblasts. The SEM/EDS and FAAS tests showed good uniformity of zinc content on a large surface of the composite. The conducted research showed the possibility of using the magnetron sputtering technique as a zero-waste method for producing antimicrobial textile composites.

Keywords: antimicrobial activity; coating; composite; cotton; cytotoxicity; magnetron sputtering; zinc

Citation: Kudzin, M.H.; Giełdowska, M.; Król, P.; Sobańska, Z. Preparation of Cotton–Zinc Composites by Magnetron Sputtering Metallization and Evaluation of their Antimicrobial Properties and Cytotoxicity. *Materials* **2022**, *15*, 2746. https://doi.org/10.3390/ma15082746

Academic Editor: Gueorgui Gueorguiev

Received: 8 March 2022
Accepted: 28 March 2022
Published: 8 April 2022

1. Introduction

Cotton is a popular fabric based on cellulose [1,2]—the most widespread biopolymer on Earth [3–5]. Consequently, the physicochemical properties of a cotton fabric follow from the cellulose polymer and depend on its chain length, topology, and surface condition [6–10]. One of the many applications of cellulose is as medical textiles, mainly wound dressings with various functions and purposes. However, the hydrophilic nature of cotton and its products, due to their large specific surface area and hydrophilicity, provide an excellent environment for the development of pathogenic microorganisms [11–13]. Therefore, antibacterial pre-functionalization of cotton intended for medical use is a standard finishing step, usually based on equipping the cotton matrix with organic/inorganic antimicrobials [12,14–16].

The wide group of these antimicrobial agents can be divided into organic (antibiotics, e.g., [17], quaternary ammonium salts [18–20], light-activated singlet oxygen generators [21,22], *N*-halamines [23]), and inorganic factors (halogens as well as heavy metals and their salts) [12,16]. Among various inorganic bactericides of medical importance, zinc is gaining more and more attention (over 5600 documents on the antibacterial activity of zinc and compounds and over 3000 on zinc oxide abstracted by Scopus) [24,25]. Zinc is indispensable in many biological processes [26], toxic to microorganisms, and nontoxic to higher organisms [27]. This chemical element is a cheap and effective antibacterial inorganic compound [14,28], due to its low cost and easy preparation [29–38], as well as antimicrobial

efficacy [29,39–44]. The chemistry of zinc is dominated by the oxidation state of (+2). Metallic zinc is a strong reducing agent (standard reduction potential $E_0 = -0.76$ V), reacting readily with acids, alkalis, and other nonmetals. The metal surface reacts with atmospheric components, thus eventually creating a protective passivating layer of basic zinc carbonate, $xZn(OH)_2/ZnOxyZnCO_3$ [45,46]. TEM studies of Zn nanoparticles (ZnNPs) showed that ZnNPs consist of a zinc core and a few nanometer thick ZnO shell [47]. Bulk oxidation of zinc in air takes place at temperatures above 450 °C [48]. The standard molar enthalpies of ZnO formation (ΔfH° solid (298.15 K·(kJ·mol^{-1})) were found to be dependent on the sample morphology, varying from −350.46 for bulk ZnO [49] to −336.57 and −343.56 for various ZnO nanoparticles [50,51]. The properties and applications of ZnO were reviewed by Ellmer and Klein [52]. Both Zn and ZnO are common target materials for magnetron sputtering-coated fabrics [53]. Strong acids, such as hydrochloric acid, remove the passivating layer, and the subsequent reaction with acid releases hydrogen gas. The predominant species in aqueous solution is the octahedral complex $(Zn(H_2O)_6)^{2+}$ [45]. The bactericidal mechanism of metal/metal oxide nanocomposites (Zn is always coated with ZnO as a result of surface passivation) consists of the production of reactive oxygen species (superoxide anions, hydrogen peroxide anions, and hydrogen peroxide) that interact with the bacterial cell wall causing damage to the cell membrane and then leakage of internal cellular components, leading to the death of bacteria [54–57]. Alternatively, ZnO-NCs in contact with bacteria release Zn^{2+} ions [29,58] which penetrate the cell membrane, destroying its normal structure and function, and consequently causing the death of bacterial organisms [59,60]. The bactericidal inactivation by ZnO performed under dark/light conditions is attributed to the bactericidal effect of Zn^{2+} ions under dark conditions or to the combined effects of Zn^{2+} ions and photocatalytically mediated electron injection under light conditions [61]. Due to the antibacterial properties of zinc oxide, several cotton–zinc oxide composites (COT–ZnO) have been proposed for medical applications [62–73]. Representative examples of antibacterial cotton using zinc salts are shown in Table 1.

Table 1. Representative composite cotton/zinc salts/MNPS.

No	Preparation	Antibacterial Activity	Ref.
2.1	COT–ZnO (Zn^{2+}(NaOH)→$Zn(OH)_2$→ZnO) ZnO deposition by 'pad–dry–cure' method.	COT–ZnO showed excellent antibacterial activity against Kp and Sa, e.g., COT–ZnO (1.6%) exhibited 99.9%rv after 24 h exposure. Application onto cotton fabrics to impart antibacterial and UV protection function.	[62]
2.2	COT–ZnO (Zn^{2+}($NH_3{}^xH_2O$)→$Zn(OH)_2$→ZnO) ZnO deposition by ultrasound irradiation.	COT–ZnO showed excellent antibacterial activity against Kp and Sa, e.g., COT–ZnO (0.8%) exhibited 99.9%rv after 2 h exposure. Potential application as coated bandages.	[63]
2.3	COT–CTS (0.3%)–ZnO (0.2–2 mM) ZnO one-step sonochemical deposition on COT/CTS	Enhanced antimicrobial effect (Sa (98.5% rv) and Ec (99.9%rv)) after 1 h incubation and high washing stability enable recommending this antibacterial textile for uses in a hospital environment to prevent the spread of nosocomial infection	[64]
2.4	COT–ZnO (0.8%) (COT + ZnO NPs (1 mM)+ C-ase (2%)), ZnO sonochemical coating.	The antibacterial efficiency of COT–ZnO (Ec 67% and Sa 100% after 1 h incubation) resisted the intensive laundry regimes used in hospitals.	[65]
2.5	COT–ZnO	In situ nanoscale synthesis of ZnO on the surface of cotton fabrics (COT + $ZnCl_2$ + NaOH→COT–ZnO) led to high antibacterial activity against Ec and Ec.	[66]
2.6	COT–ZnO; COT–PVP–ZnO	The antibacterial efficiency of COT–ZnO after 2 h incubation: COT–ZnO (5 mg/L)—Ec, 81%rv and Sa, 57%rv; COT–PVP–ZnO (5 mg/L)—Ec, 80%rv and Sa, 71%rv; COT–PVP–ZnO (20 mg/L)—Ec, 100%rv and Sa, 100%rv. Potential application as wound cloths, surgical cloths, sportswear and kidswear.	[67]

Table 1. *Cont.*

No	Preparation	Antibacterial Activity	Ref.
2.7	COT–R–N^+Me_3_ZnO/ZnO	Nano-ZnO films deposited on cotton fabrics (10–16 layers) exhibited excellent antimicrobial activity against Sa.	[68]
2.8	COT–ZnO; COT–BTCA–SiO_2–ZnO; COT–APTES–BTCA–SiO_2–ZnO; COT–VTES–SiO_2–ZnO;	The antibacterial efficiency of hybrids varied for Ec from 96%rv to 99%rv and for Sa from 55%rv to 90%rv; after 20 washing cycles, it varied for Ec from 57%rv to 91%rv and for Sa from 55%rv to 90%rv. Multi-application potential.	[69]
2.9	COT–ZnO (Zn^{2+}(HMTETA, H_2O)→ZnO)	The antibacterial efficiency of hybrids after 24 h exposure varied for Ec from 91%rv to 97%rv and for Sa from 95%rv to 98%rv.	[70]
2.10	COT–ZnO (Zn^{2+}(MMA, EtOEtOH)→ZnO) ZnO coating by a spin coater.	The antibacterial activities of the ZnO-coated fabric were investigated (zone inhibition diameter) against Kp, St (36 mm), Ec (19 mm), Bs (17 mm), and St (20 mm) using 48 h exposure time. Comparable with ampicillin and/or gentamycin.	[71]
2.11	COT–ZnO (Zn^{2+}(H_2O, NH_4Cl, NH_3)→ZnO) ZnO synthesized on the surface of COT via a simple wet chemical route.	Antibacterial tests against Sa and Kp (the presence of a significant inhibition zone of at least 1 mm around the fabric) revealed good bacteriostatic activity. However, the negligible reduction in the number of bacteria proved the lack of bactericidal activity.	[72]
2.12	COT–ZnO (1%) (Zn^{2+} (H_2O, At)) ZnO resuspended in water (20 ppm) was coated on cotton.	The treatment of the cotton fabrics with ZnO-NPs was carried out at a safe dose (20 ppm). At this dose, ZnO-NP-loaded samples exhibited reasonable antibacterial activity against Sa, Bs, Ec, and Pa.	[73]

Bacteria and fungi: At—Aspergillus terreus AF-1; Bs—Bacillus subtilis; Ca—Candida albicans (fungi); Ec—Escherichia coli; Kp—Klebsiella pneumoniae; Pa—Pseudomonas aeruginosa; Sa—Staphylococcus aureus; St—Salmonella typhimurium; %rv—percentage reduction in viability of bacteria/fungi. Reagents: APTES—(3-aminopropyl) triethoxysilane; BTCA—butyltetracarboxylic acid; VTES—vinyltriethoxysilane; HMTETA—hexamethyltriethylene tetramine; MMA—monomethyl amine, EtOEtOH—ethoxyethanol. Fibers/textiles: COT—cotton, CTS—chitosan.

The modification of textiles by means of magnetron sputtering does not require the use of any chemicals, can be achieved in one process cycle in a single industrial installation, and does not involve the emission of toxic substances to the environment or the production of pollutants [53,74–80]. Therefore, this method can be considered eco-friendly and zero-waste.

Zinc magnetron sputtering is one of the techniques frequently used in modern science and technology (11,739 documents on zinc sputtering abstracted by Scopus [81]), as well as in relation to sputtering of zinc on polymers (283 documents on polymer zinc sputtering [82]). Thus, zinc oxide (ZnO) films have been deposited on polyethylene terephthalate (PET) [83–91], polyethylene naphthalate (PEN) [79,83,92,93], polytetrafluoroethylene (PTFE) [94–97], and poly(acrylic acid) [98], as well as on the surface of polypropylene (PP) fibers [99], polystyrene [100], and poly(ether ether ketone) (PEEK) films [101].

Only a few studies have been devoted to other zinc compounds such as zinc sulfide (ZnS) deposited on polyethylene terephthalate (PET) [102] and gallium-doped zinc oxide (GZO) deposited on a transparent flexible substrate based on cellulose derivatives [103]. Only in two studies was metallic zinc used for surface functionalization of polymer nanofibers, namely, for polyamide [104], and for polyethylene (PE) and polytetrafluoroethylene (PTFE) [105].

As part of our research program dedicated to biologically active functionalized phosphonates [106,107] and biofunctionalization of textile materials [108–114], we present the preparation and physicochemical and biological properties of the COT–Zn polymer hybrid. The aim of this work was to modify the surface of cotton fabric with zinc using the DC (direct current) magnetron sputtering method to produce a new antimicrobial, multifunctional composite material.

2. Materials and Methods

2.1. Materials

2.1.1. Composite Components

- Medical fabric with a plain weave; qualitative composition: cotton (100% *w*/*w*); weight: 200 g/m^2 (Andropol S.A., Andrychów, Poland);
- Zinc sputtering target with 99.9% purity with a rectangular size (798 × 122 × 6 mm) (Testbourne Ltd., Basingstoke, UK).

2.1.2. Bacterial and Fungal Strains

The following bacterial strains and fungal strains were purchased from Microbiologics (St. Cloud, MN, USA):

- *Escherichia coli* (ATCC 25,922, Microbiologics, St. Cloud, MN, USA);
- *Staphylococcus aureus* (ATCC 6538, Microbiologics, St. Cloud, MN, USA);
- *Aspergillus niger* (ATCC 6275, Microbiologics, St. Cloud, MN, USA);
- *Chaetomium globosum* (ATCC 6205, Microbiologics, St. Cloud, MN, USA).

2.1.3. Cell Culture

BALB/3T3 clone A31 cell line cat. no. CCL-163 (mouse fibroblasts) was purchased from the American Type Culture Collection/the Global Bioresource Center (ATCC, Manassas, VA, USA).

2.2. Methods

2.2.1. Magnetron Sputtering

The medical cotton fabric (COT) was modified using a DC (Direct Current) magnetron sputtering system produced by P.P.H. Jolex s.c. (Czestochowa, Poland) and a zinc target. The distance between the target and the substrate was 15 cm. The deposition of coatings was carried out in the atmosphere of argon. The following parameters were used for the modification: discharge power 700 W, with the resulting power density 0.72 W/cm^2 and working pressure 2.0 × 10^{-3} mbar. In order to differentiate the zinc content ($Zn^{(0)}$ + $Zn^{(2+)}$) in the composites COT–Zn, three different deposition variants were used, i.e., 5 min one-sided (sample name: COT–Zn-5(1 s)), 10 min one-sided (COT–Zn-10(1 s)), and 10 min two-sided (COT–Zn-10(2 s)).

2.2.2. SEM/EDS—Scanning Electron Microscopy/Energy-Dispersive X-ray Spectroscopy

The microscopic structure was examined using a HITACHI S-4700 scanning electron microscope (Tokyo, Japan) equipped with a Thermo NORAN EDS X-ray microanalyzer (Waltham, MA, USA). The topography analysis of the tested samples was carried out in low vacuum at a beam energy of 10 kV and magnifications of 400×, 1600×, and 3000×. The study was conducted under low vacuum in the presence of steam. Water vapor dissipates excess charge, making it possible to image nonconductive materials without coating the surface with gold.

2.2.3. Atomic Absorption Spectrometry with Flame Excitation—FAAS

Zinc content in the composite samples was determined using the Thermo Scientific Thermo Solar M6 atomic absorption spectrometer (Waltham, MA, USA) equipped with a 100 mm titanium burner, coded lamps with a single-element hollow cathode, and a D2 deuterium lamp for background correction. The sample was prepared using a single-module Magnum II microwave mineralizer from Ertec (Wroclaw, Poland).

The total zinc content of the sample *M* (mg/kg) was calculated according to the following formula [115]:

$$M = \frac{C_i \times V}{m} \left[\frac{\text{mg}}{\text{kg}}\right], \quad (1)$$

where C is the Zn concentration in the tested solution (mg/L), m is the mass of the mineralized sample (g), and V is the volume of the sample solution (mL).

2.2.4. Biological Experiments

Antibacterial Activity

The antibacterial activity of COT–Zn composites was tested by the agar (Mueller Hinton medium) diffusion method (PN-EN ISO 20,645:2006), on colonies of Gram-negative (*E. coli*; ATCC 25,922) and Gram-positive (*S. aureus*; ATCC 6538) bacteria [116]. The test was initiated by pouring each agar into sterilized Petri dishes and allowing it to solidify. The surfaces of agar media were inoculated with the overnight broth cultures of bacteria (ATCC 25,922: 1.5×10^8 CFU/mL, ATCC 6538: 2.5×10^8 CFU/mL). Samples of sterile COT–Zn discs and a control, unmodified sample (10 mm) were placed on the inoculated agar and incubated at 38 °C for 24 h. The diameter of a clear zone around the sample was measured as an indication of inhibition of the microbial species. All tests were carried out in duplicate.

Antifungal Activity

The antifungal activity of the COT–Zn composites was tested according to PN–EN 14,119:2005 against *A. niger* (ATCC 6275) and *C. globosum* (ATCC 6205) [117]. Specimens of the tested material were placed on agar plates; the samples of sterile modified COT–Zn discs (20 mm) and the control, unmodified sample were placed on inoculated agar (pH:6.2) and incubated at 30 °C for 14 days. The agar was inoculated with the selected fungus (ATCC 6275: CFU/mL = 3.5×10^6, ATCC 6205: CFU/mL = 3.0×10^6). The level of antifungal activity was assessed by examining the extent of fungal growth: in the contact zone between the agar and the specimen, on the surface of specimens, and, if present, the extent of the inhibition zone around the specimen. All tests were carried out in duplicate.

2.2.5. Cytotoxicity

Cell Culture

Cells (mouse fibroblasts: BALB/3T3 clone A31 cell line cat. no. CCL-163) were grown in T-25 culture flasks in a humidified CO_2 incubator (37 °C, 5% CO_2) and maintained in a culture medium (cDMEM), i.e., DMEM medium (Biowest, Riverside, CA, USA) with 10% fetal bovine serum (Gibco, Waltham, MA, USA), 100 U/mL penicillin, 100 µg/mL streptomycin (Biowest, Riverside, CA, USA), 4 mM L-glutamine (Biowest, Riverside, CA, USA), and 20 mM HEPES (Sigma-Aldrich, Saint Louis, MO, USA). Cells were examined daily using an Olympus IX70 inverted microscope (Tokyo, Japan) and were routinely passaged twice a week when reaching 60–70% confluency. Next, they were detached using 0.25% trypsin-EDTA solution (BI, Kibbutz Beit-Haemek, Israel) (5 min, 37 °C) and seeded in 96-well plates (3.5×10^3 cells/well). Then, the cells were allowed to adhere for 22–24 h in the CO_2 incubator.

Extract Preparation and Cell Treatment

Extracts of test materials (COT and COT–Zn composites) were prepared according to EN ISO 10993-12-2012 [118] using the exposure medium, i.e., cDMEM with a lower (5%) concentration of FBS, in order to avoid the masking of toxicity by the protective effect of the serum. Test materials were autoclaved (120 °C, 20 min) and left at 70 °C for 5 h to dry. Next, the materials were immersed in the exposure medium using the extraction ratio of 0.1 g of the material to 1 mL of the exposure medium, i.e., the predetermined additional volume of the exposure medium needed for the maximum soaking of the test material. Extraction was performed in shaken vials that were incubated at 37 °C for 24 h. The pH values of extracts (ca. 8) were adjusted to 7.4 using 1 N HCl (POCH, Gliwice, Polska). Extracts, the preparations, and sample abbreviations are summarized in Table 2.

Table 2. Extract abbreviations.

Extracts Abbreviations	Starting Materials				Exposure Medium (NC) [a]	
	COT	COT–Zn [b]	E-COT (100%)	E-COT–Zn (100%)	Extraction [c]	Dilution
E-COT (100%)	0.1 g				1.n_1 mL	
E-COT (50%)			0.5 mL			0.5 mL
E-COT–Zn (100%)		0.1 g			1.n_2 mL	
E-COT–Zn (50%)				0.5 mL		0.5 mL
E-COT–Zn (25%)				0.25 mL		0.75 mL

[a] cDMEM with a lower (5%) concentration of FBS; [b] COT–Zn-10 (1 s) was used for cytotoxicity assays; [c] 1 mL of the exposure medium + the predetermined additional volume of the exposure medium needed for the maximum soaking of the test material (ni).

Cells were exposed to the extracts at selected concentrations (100% and 50% for unmodified cotton; 100%, 50%, and 25% for modified cotton) for 24 h, i.e., after 24 h adherence of cells, the supernatant above the cells was aspirated and replaced with 100 µL of an appropriately concentrated extract or control solution (negative control, NC—exposure medium treated in the same way as extracts; positive control—SDS (Sigma-Aldrich, Saint Louis, MO, USA) in the concentration range 0–150 µg/mL). During the experiment cells were examined with the Olympus IX70 (Tokyo, Japan) inverted microscope. Each sample was tested in triplicate per experiment, and three independent experiments were performed.

The Neutral Red Uptake (NRU) Assay

After the 24 h incubation of BALB/3T3 clone A31 cells with the extracts, the medium was gently aspirated, and the wells were washed with 150 µL of Dulbecco's phosphate-buffered saline (PBS) with Ca^{2+} and Mg^{2+} ions (BI, Kibbutz Beit-Haemek, Israel). Then, 100 µL of NR (Sigma-Aldrich, Saint Louis, MO, USA) solution (50 µg/mL, prepared in culture medium) was added to each well, and the plates were incubated further for 3 h (37 °C; 5% CO_2). Afterward, the NR solution was removed, the wells were washed with 150 µL of PBS, and 150 µL of desorbing solution [1% glacial acetic acid (POCH, Gliwice, Polska), 50% ethanol (POCH, Gliwice, Polska), and 49% deionized water] was added to each well. Absorbance was read at 540 nm using a Multiskan™ GO spectrophotometer (Thermo Fisher Scientific, Waltham, MA, USA). Results were expressed as the percentage cell survival (OD of exposed vs. OD of control unexposed cells).

3. Results and Discussion

3.1. SEM/EDS—Scanning Electron Microscopy/Energy-Dispersive X-ray Spectroscopy

The analysis of changes in the morphological structure of fibers in cotton fabric under zinc modification was carried out using scanning electron microscopy. Figure 1 shows SEM images of the samples before and after magnetron sputtering, at magnifications of 400×, 1600×, and 3000×.

According to the image analysis, it can be noted that the fibers in cotton fabric were characterized by a rather smooth surface with characteristic parallel ridges and grooves. The fibers in cotton fabric with a magnetron-sputtered zinc layer were characterized by a rougher surface with visible ridges and grooves in the fibers. The zinc coating exhibited a regular distribution of the applied modifier particles.

In order to confirm and verify the uniformity of the zinc coating of the fibers, an energy-dispersive X-ray spectroscopy (EDS) study was performed, which provided a chemical analysis of the tested fabric and its elemental composition. The EDS surface analysis (Figure 2) in the form of individual "mapping" and the quantitative spot analysis showed the content of characteristic elements in the cotton fiber surface.

The study indicated a uniform distribution of zinc on the surface-modified fibers. The black areas visible in the images were the spaces between the fibers in the yarn (three-dimensional structure). Due to the dense and uniform zinc coating of the fibers, carbon

became less visible, which was confirmed by the quantitative analysis of the content of elements on the fiber surface (Table 3) and EDS punctate analysis diagram (Figure 2).

Table 3. Quantitative content of elements in individual samples based on the EDS test.

Sample	Quantitative Content of Elements (wt.%)		
	C	O	Zn
COT	40.04	59.96	-
COT–Zn-10 (1 s)	3.20	17.70	79.73

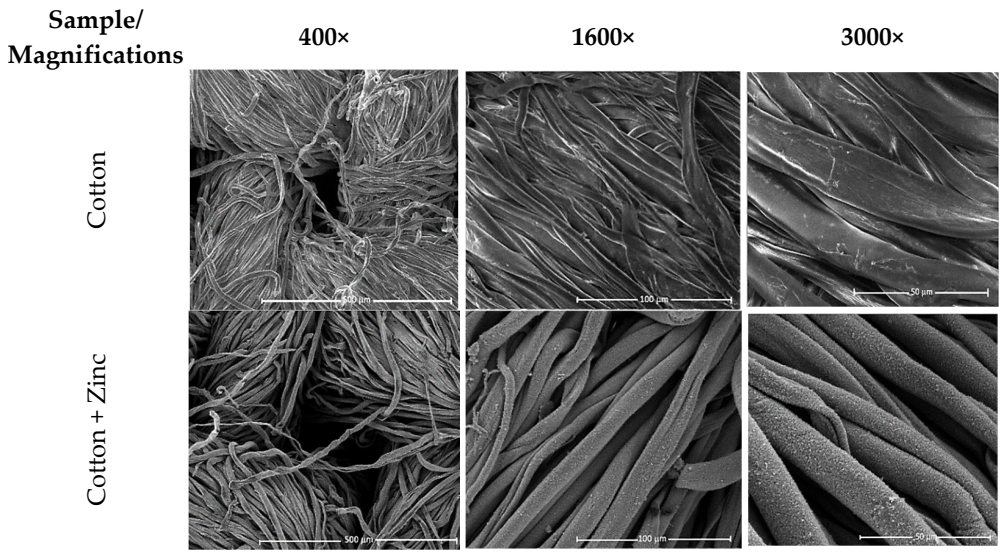

Figure 1. SEM results (magnifications: 400×, 1600×, and 3000×) of the tested samples recorded before and after magnetron sputtering with a zinc target.

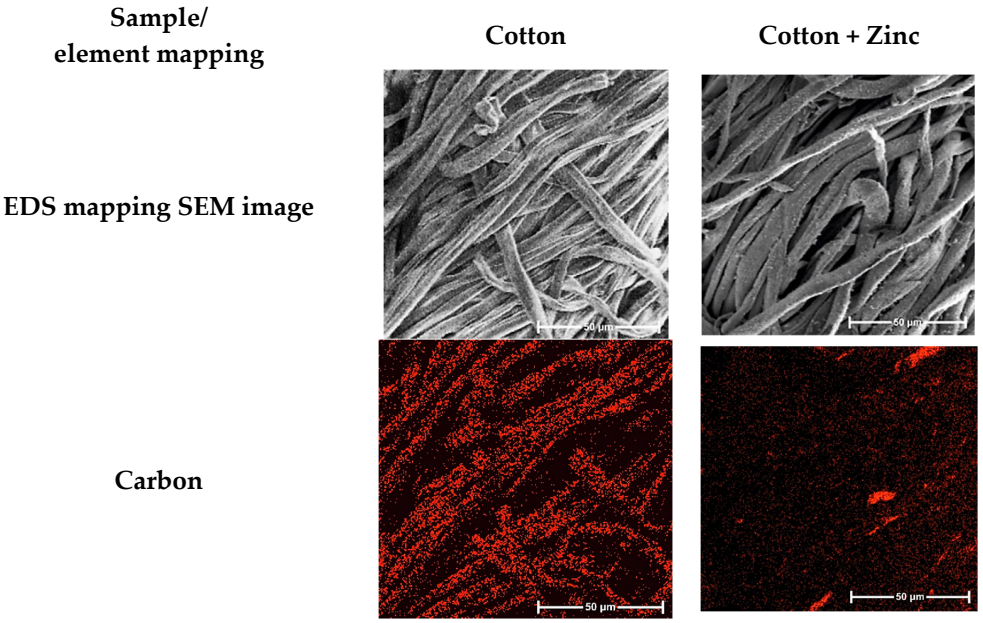

Figure 2. *Cont.*

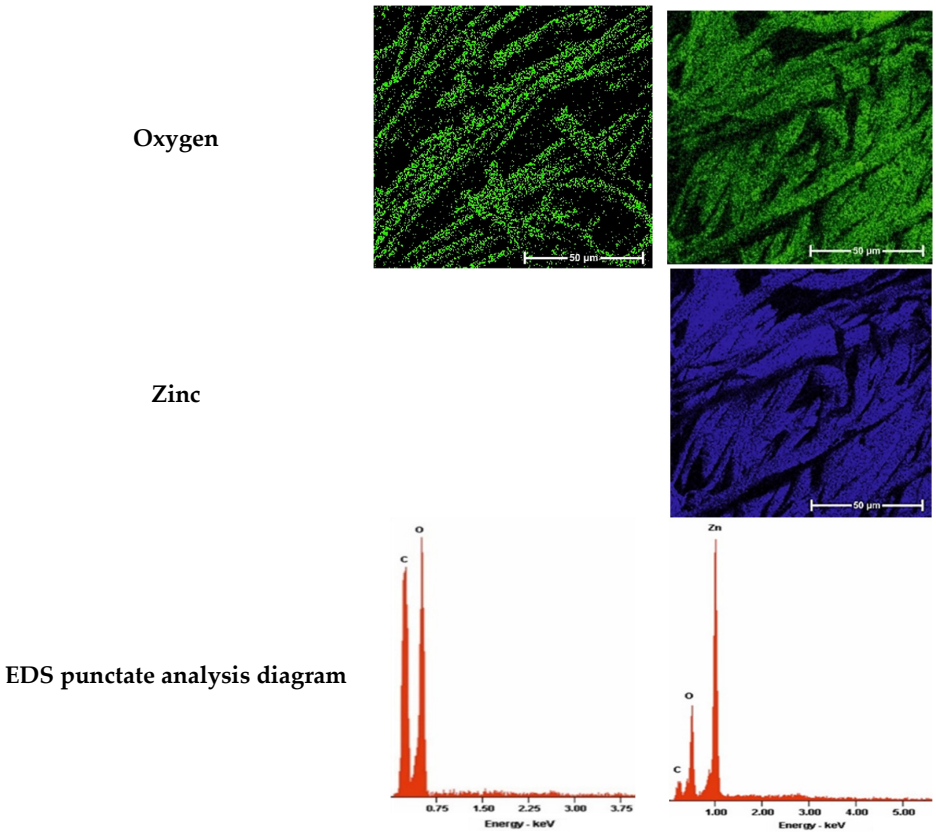

Figure 2. Multi-element EDS mapping images and EDS spot analysis diagram: analysis of the chemical composition of COT and COT–Zn sample.

The nature of the so-called zinc–cellulose interface matter (Zn–cell–OH) still remains unclear, since the zinc atom is reactive, and cellulose possesses reactive hydroxyl functions. It is well documented that zinc reacts with alcohols with the temporary formation of zinc alcoholate intermediates, which, in an aqueous environment, rearrange into zinc oxide [119–122].

The reactions of zinc with alcohols presumably proceeded in accordance with Figure 3.

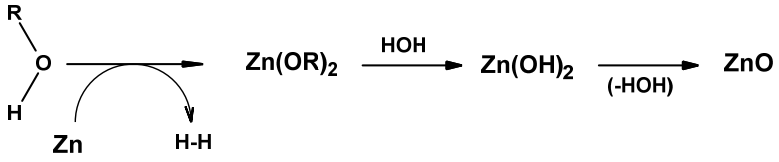

Figure 3. Putative mechanism of the reaction of zinc with alcohols (R = Me or Et) [119–122].

Subsequently, zinc atoms of a metallic monolayer deposited on the cellulose surface reacted during deposition with cellulose, forming corresponding alcoholates (Figure 4), which could subsequent hydrolyze to cellulose and ZnO.

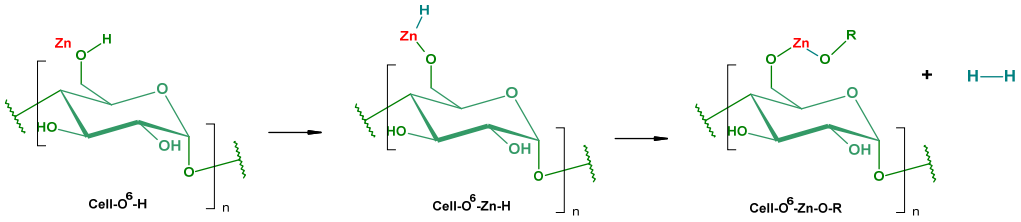

Figure 4. Putative mechanism of the reaction of zinc with cellulose during sputtering deposition of zinc on cotton.

The following layers of deposited zinc atoms were attached to the lower zinc layer, forming appropriate zinc multilayers. The zinc atoms of the upper layer were oxidized to ZnO, by reaction of zinc atoms with oxygen or water. This mechanism was partly confirmed by EDS test (Table 3). The results for COT were as follows: C (40.0%), O (60.0%); the results for COT–Zn-10 (1 s) were as follows: C (3.2%), O (17.7%), Zn (79.7%). This suggests that carbons of the cellulose skeleton were covered by O–Zn moieties. Cellulose-derived oxygens were masked by zinc atoms; hence, the oxygen revealed in the EDS test was presumably derived from the passivated layer, i.e., from ZnO. The ratio of Zn:O ≈ 4.5:1 ($Zn_{1.2}O_{1.1}$) suggests a nearly quantitative character of passivation. It is worth adding that the formation of ZnO during sputtering with pure zinc has been described in a few papers using pure Zn target in an argon–oxygen [123–125] or oxygen atmosphere [126]. Another example of the formation of a metal–polymer interface during Zn sputtering onto PE, PTFE, and PI surfaces was described by Pertsin and Volkov [105].

3.2. Atomic Absorption Spectrometry with Flame Excitation—FAAS

The determination of zinc content in COT–Zn composite samples was assessed by the FAAS method, and the results are presented in Table 4.

Table 4. Results of determination of zinc content in COT–Zn composite samples.

Sample Name	Zn Concentration (g/kg)
COT	0.01
COT–Zn-5 (1 s)	9.06
COT–Zn-10 (1 s)	20.19
COT–Zn-10 (2 s)	41.52

The results were measured in triplicate and are presented as mean values with a deviation of approximately ±2%.

The zinc content in composite samples strictly depended on the applied sputtering metallization times. The process of Zn deposition on the cotton sample was practically linear (COT–Zn-5 (1 s)—9.06 g/kg, COT–Zn-10 (1 s)—20.19 g/kg, COT–Zn-10 (2 s)—41.52 g/kg), and the distribution of metal in COT–$Zn^{(0)}$ material bulk after modification was uniform.

3.3. Antimicrobial Properties

3.3.1. Antibacterial Activity

The COT–Zn composites were tested in vitro for antimicrobial activity against Gram-positive *S. aureus* and Gram-negative *E. coli*. Results of the tests are illustrated in Figures 5 and 6.

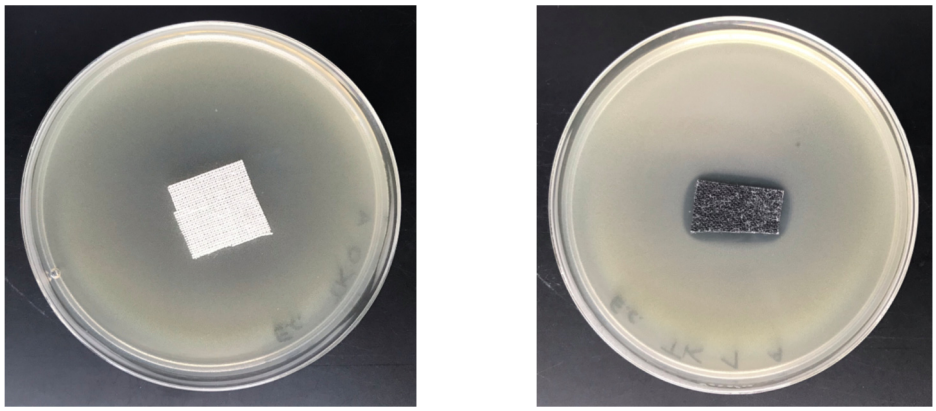

(**a**) (**b**)

Figure 5. Tests of antimicrobial activity of COT–$Zn^{(0)}$ composites against *E. coli*. Inhibition zones of bacterial growth in Petri dishes: (**a**) COT; (**b**) COT–Zn-10 (1 s/2 s).

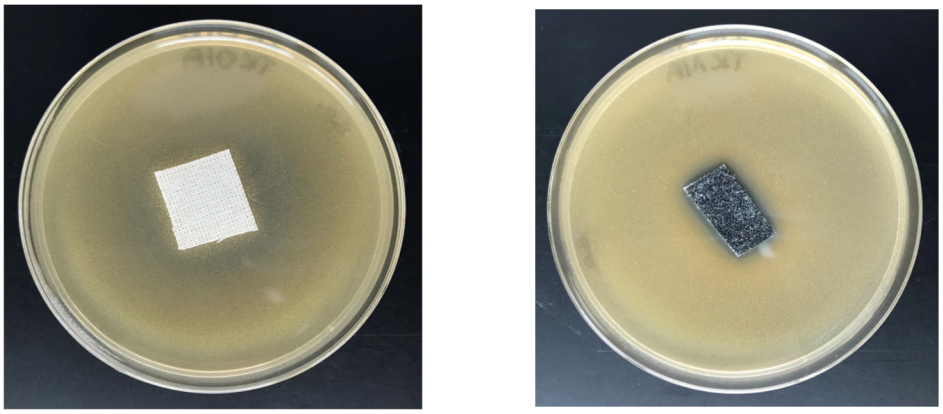

(**a**) (**b**)

Figure 6. Tests of antimicrobial activity of COT–$Zn^{(0)}$ composites against *S. aureus*. Inhibition zones of bacterial growth in Petri dishes: (**a**) COT; (**b**) COT–Zn-10 (1 s/2 s).

A comparison of these results (ZID) with representative data from the literature is given in Table 5.

Table 5. Results of antibacterial activity test of zinc compounds and composites.

Sample	Conc.	Zone Inhibition Diameters (mm) [/a]								Ref.
		Gram-Negative				Gram-Positive				
		Ec	Kp	Pa	Pm	Bs	Ef	Sa	Se	
$ZnSO_4$	2 mg/mL	17	14	14	15			28	15	[127]
$ZnSO_4$	10 mg/mL	23	26	21	23			38	26	
ZnO NPs	1 mg/mL	16				19		18		[128]
ZnO NPs	1 mg/mL	18						15		[129]
ZnO (ZOE)							3			[130]
$ZnCl_2$	6 mg/mL	-	-		-	-		-		
$Zn(L^i)_2(W)_2$	6 mg/mL	-	-		-	10		12		[131]
$Zn(L^i)_2(L^2)(W)_2$	6 mg/mL	14	11		14	12		15		
ZnO NPs	50 µg/mL	24	16	26		24		22		[132]
COT [/b]	0.01 mg/g	0						0		
COT–Zn-5 (1 s) [/b]	9.0 mg/g	1						0		This work [/c]
COT–Zn-10 (1 s) [/b]	20 mg/g	1						1		
COT–Zn-10 (2 s) [/b]	42 mg/g	1						1		

[/a] Zone inhibition diameter (ZID), rounded to whole numbers (mm); NPs—nanoparticles; L—ligand (L1= ibup (ibuprofen); L2 = 2′-bipy (2,2′-bipyridine); W = water); ZOE—ZnO–eugenol. [/b] Concentration of inoculum: *E. coli*: CFU/mL = 1.5×10^8, *S. aureus*: CFU/mL = 2.5×10^8. [/c] ZID determined according to PN-EN ISO 20,645:2006 standard [116]. Bacteria: Bs—*Bacillus subtilis*; Ec—*E. coli*; Ef—*Enterococcus faecalis*; Kp—*Klebsiella pneumoniae*; Pa—*Pseudomonas aeruginosa*; Pm—*Proteus mirabilis*; Sa—*Staphylococcus aureus*; Se—*Staphylococcus epidermis*.

The literature data related to the antibacterial activity of zinc-based composites cannot be used as direct comparative data, due to the difference in the applied test methods. The presented results (Table 5) indicate that, independently of the type of base material used for modification with Zn and zinc compounds, and irrespective of the applied test method to evaluate antimicrobial activity, the expected result was achieved. Results of these tests demonstrate the antimicrobial protection against various bacterial microorganisms of COT–Zn-10 (1 s/2 s) composites for *E. coli* and *S. aureus* (Table 5), expressed by the visible zones of inhibition of bacterial growth on the Petri dishes (Figures 5b and 6b).

3.3.2. Antifungal Activity

The results of the antifungal activity tests (ZID) in accordance with PN-EN 14119:2005 against colonies of *A. niger* (ATCC 6275) and *C. globosum* (ATCC 6205) for the cotton

sample and COT–Zn composites are illustrated in Figures 7 and 8 and presented in Table 6 (comparison with representative data from the literature).

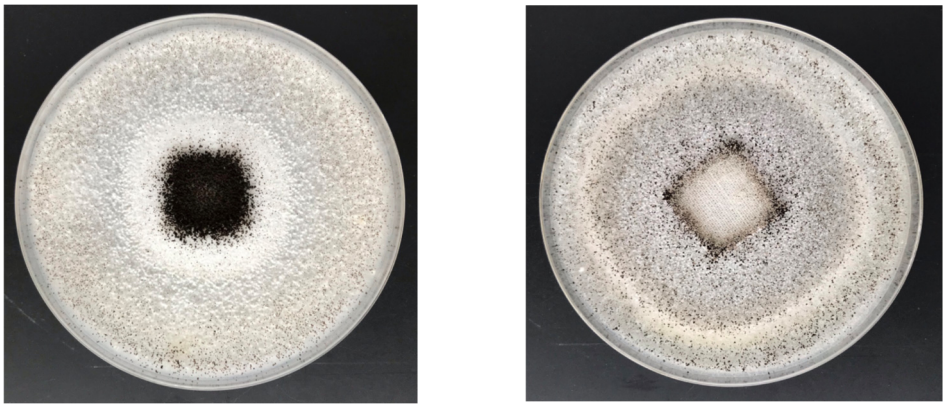

(**a**) (**b**)

Figure 7. Antimicrobial activity tests against *A. niger*. Inhibition properties of fungal growth in Petri dishes: (**a**) COT; (**b**) COT–Zn-10 (1 s/2 s).

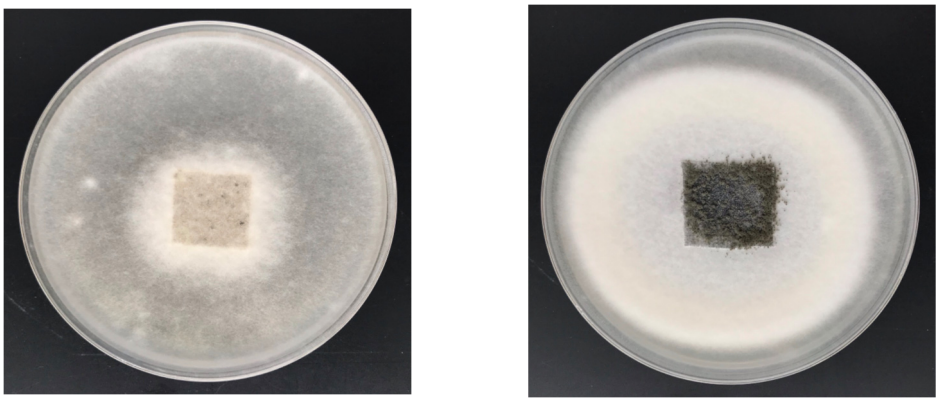

(**a**) (**b**)

Figure 8. Antimicrobial activity tests against *C. globosum*. Inhibition properties of fungal growth in Petri dishes: (**a**) COT; (**b**) COT–Zn-10 (1 s/2 s).

Table 6. Results of the antifungal activity test and growth inhibition effects of zinc compounds and composites.

No	Zinc Compounds/Composites [a]	Deposition [b]	Fungal Average Zone Inhibition Diameters (ZID: mm) [c,d]					Ref.
			An	Afl	Afu	Ca	Cg	
1	ZnO	1 mg/mL	8	8				[133]
		1 mg/mL	18			20		[134]
	ZnO NPs	0.4 mg/mL	35					[135]
		50 µg/mL	16			19		[132]
	ZnO NPs	1 µg/mL	24			28		[136]
2	$Zn(OAc)_2$	1 µg/mL	20			21		
		1 mg/disc	6	8	6			[137]
		10 mg/disc	8	11	8			
	ZnO NPs	0.02 mg/mL	10	5	7	14		[138]
		0.1 mg/mL	13	10	11	19		
		/e	0–9 /e,f			0–8 /e		[139]

Table 6. *Cont.*

No	Zinc Compounds/Composites [/a]	Deposition [/b]	Fungal Average Zone Inhibition Diameters (ZID: mm) [/c,d]					Ref.
			An	Afl	Afu	Ca	Cg	
3	ZnO/CuO (1:1) NPs	0.5 mg/mL	0	0				[140]
4	hAp	5µg	12			13		[141]
	hAp–Zn (15%)	5µg	12			18		
5	Cell/Cts/ZnO	0.25%	9–11					[142]
6	CTS–ZnO film	1 mg/mL	14			4		[143]
7	PS/ZnO-NPs (5%)		19	20				[144]
8	ZnO NPs–eugenol	26 µg/L	24					[145]
9	PLA–ALG–Zn^{2+}	1.2%	1				1	[146]
	PLA–ALG–Zn^{2+}	4.0%	1				1	
10	COT–ZnO	[/f]	10					[147]
	COT–ZnO–MnO_2(1:1)	[/f]	12					
11	COT [/b]	0.01 mg/g	0 [/g,h]				0 [/g,h]	This work
	COT–Zn-5 (1 s) [/b]	9.0 mg/g	0 [/g,h]				0 [/g,h]	
	COT–Zn-10 (1 s) [/b]	20 mg/g	1 [/g,h]				1 [/g,h]	
	COT–Zn-10 (2 s) [/b]	42 mg/g	1 [/g,h]				1 [/g,h]	

[/a] Zinc compounds and composites; Cell—cellulose; COT—cotton; Cts—chitosan; hAp—hydroxyapatite; PLA—polylactide; PS—polystyrene; ZnO NPs—zinc oxide nanoparticles. [/b] Deposited on discs as originally assigned (ug/mL, mg/mL, mg/disc; % of zinc in the solution or solid sample). [/c] Fungi: An—*Aspergillus niger*; Afl—*Aspergillus*; Afu—*Aspergillus fumigates*; Ca—*Candida albicans*; Cg—*Chaetomium globosum*. [/d] Zone inhibition diameter (ZID), rounded to whole numbers (mm); ZID was determined according to PN-EN ISO 20,645:2006 standard [117]. [/e] Dependent on the green method applied. [/f] Dependent on the green method applied. [f] Cotton patch (5 × 5 cm^2) saturated for 5 min in 10% aqueous solution of ZnO and/or MnO_2/ZnO. [/g] Concentration of inoculum: *A. niger*: CFU/mL = 3.5 × 10^6, *C. globusum*: CFU/mL = 3.0 × 10^6. [/h] Visible growth on sample surface.

As anticipated, the unmodified sample (100% cotton) did not inhibit the growth of *A. niger* or *C. globosum*, as expressed by the strong visible fungal growth covering the entire surface of the COT samples (Figures 7a and 8a). Antifungal activity and protection against *A. niger* and *C. globosum* were demonstrated by COT–Zn-10 (1 s/2 s) samples modified by magnetron sputtering metallization. The results revealed visible zones of fungal growth inhibition in Petri dishes (Figures 7b and 8b), with no fungal growth on the surface of the composites.

The zinc oxide impact on bacteria or fungi depends on its morphology (particle size and shape), concentration, exposure time, pH, etc. [148]. This is illustrated by the corresponding ZID values summarized in Tables 5 and 6. Generally, ZnO NPs had ZID values over 10 mm, revealing the dependence of antimicrobial activity on zinc concentration (ZID = f(ZnX)). In a few cases, the ZnO NP ZIDs were comparable with the ZIDs of precursory zinc salts ($ZnCl_2$, $ZnSO_4$, or $Zn(OAc)_2$). Since zinc metal presents lower solubility than ZnO (1 µg/L vs. 3.6 µg/L) [149] and much lower solubility than ZnO NPs [150–153], the metallic zinc in COT–Zn composites presented lower solubility in inoculum media than ZnO NPs and, consequently, a lower ZID. Therefore, the process of releasing antimicrobial zinc ions from COT–Zn (COT–Zn→COT–$Zn(OH)_2$→COT + Zn^{2+}) is much longer, and these composites should preserve their antimicrobial nature/characteristics for much longer.

3.4. Cytotoxicity

Cytotoxicity assays [154–156] are crucial in biomaterial science with respect to the therapeutic potential of nanocomposites and nanostructures, as well as the legal and normative requirements for medical devices and biomaterials [157–164]. These include an array of methods, mostly fluorescent and colorimetric, providing quantitative estimations of the number of viable cells in a culture [154,155]. The neutral red uptake (NRU) assay is one of the most used cytotoxicity tests in biomedical and environmental applications [165] and is based on the natural tendency of neutral red dye to incorporate to living cell lysozymes.

As cells begin to die (a loss of cell viability), their ability to bind neutral red diminishes (decrease in neutral red uptake), corresponding to colorimetric changes.

Zinc salts have proven to exert a strong biological effect, i.e., an antimicrobial effect toward several bacteria [41], as well as a cytotoxic effect toward various mammalian cell viability [166]. Cytotoxicity studies were used to screen the therapeutic potential of zinc-containing nanostructures [167–175]. Zn/ZnO coatings are partially soluble in water [149], releasing Zn^{2+} ions. These, in turn, induce cytotoxicity by increasing the excessive intracellular Zn ion concentration [166,176,177]. In order to screen the therapeutic potential of COT–Zn composites, we investigated their cytotoxic action on Balb/c 3T3 fibroblast cells [178], using the neutral red uptake assay [174,178].

3.5. Cytotoxicity Experiments

Macroscopic observations of the extracts showed no changes in transparency for unmodified cotton, while the modified cotton had a visibly darker color, brightening after sedimentation, and leaving a black residue (Figure 9A.). Microscopic analysis of the exposed cells revealed fibers present in all extract samples and small fragments present only in the modified cotton extracts (Figure 9B).

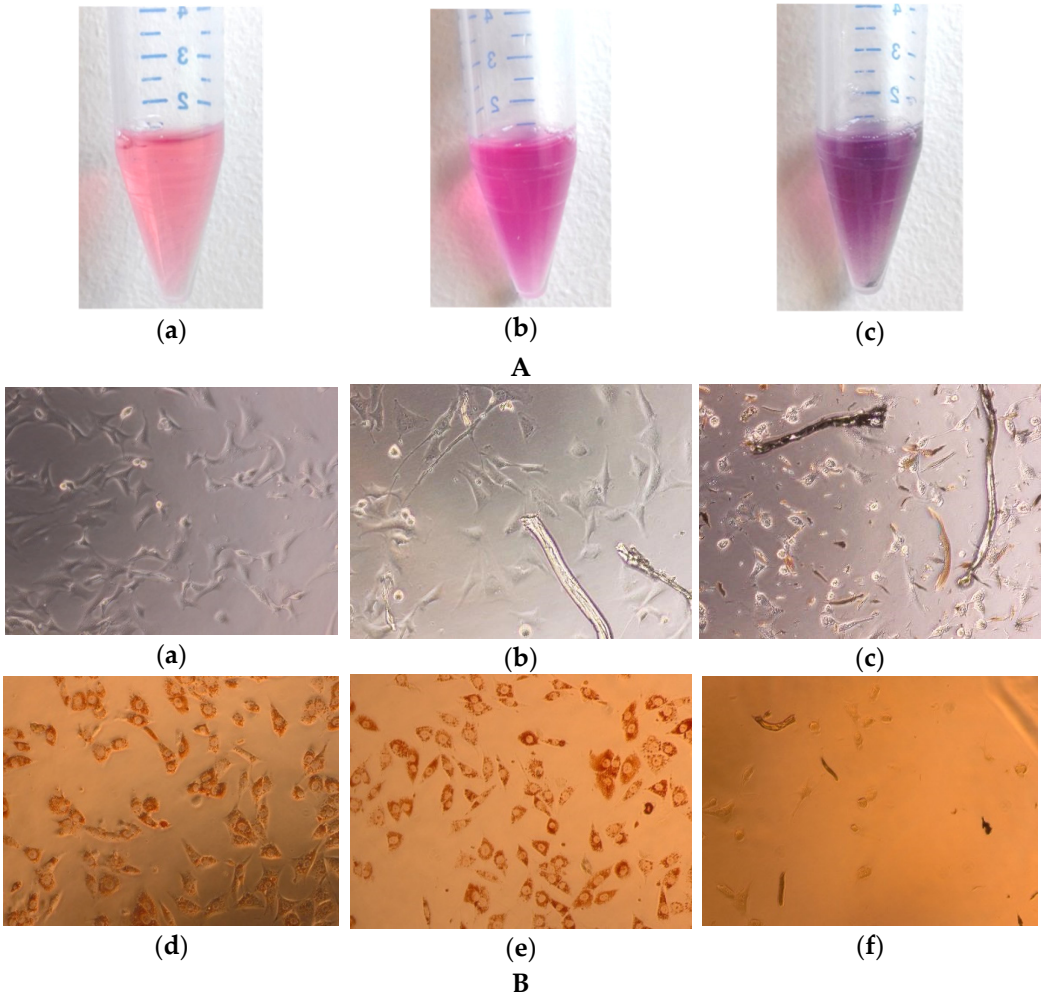

Figure 9. (**A**). Images showing exposure medium treated in the same way as (NC) extracts (**a**), unmodified cotton extract (**b**), and modified cotton extract (**c**), (**B**). Light microscopy images of BALB/3T3 clone A31 cells exposed for 24 h to negative control (**a**,**d**), 100% unmodified cotton extract (**b**,**e**), and 100% extract from COT–Zn sample (**c**,**f**), before and after incubation with NR, respectively.

The results of the NRU assay showed no decrease in viability of fibroblasts exposed to the unmodified cotton extracts at both tested concentrations. COT–Zn extracts significantly

reduced cell viability, causing almost 100% cell death, irrespective of the extract concentration (Figure 10). Treatment of cells with SDS resulted in a concentration-dependent decrease in cell viability (Figure 11).

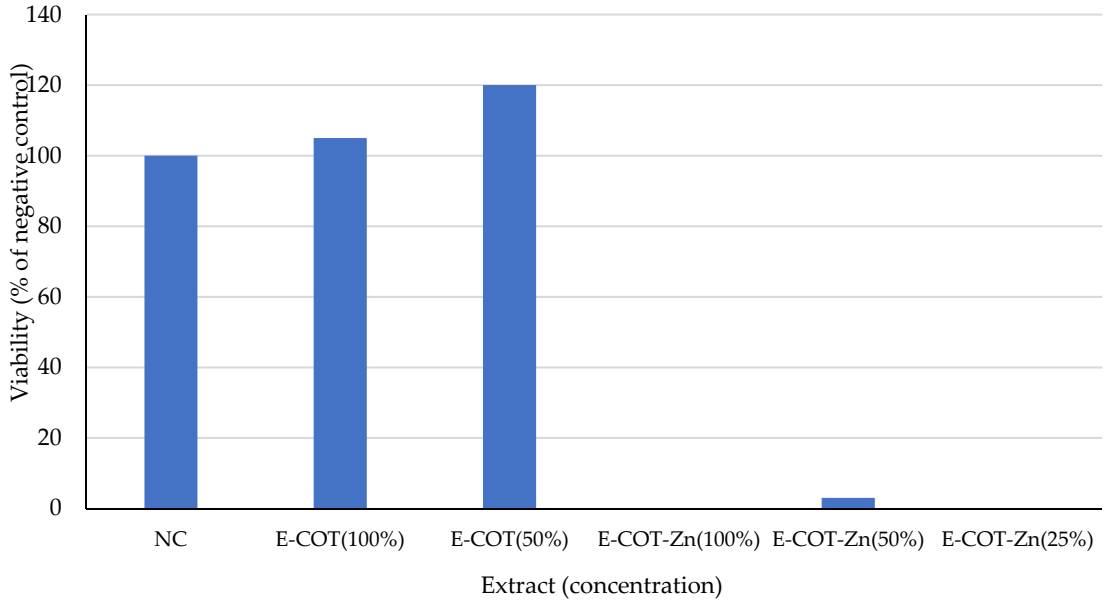

Figure 10. Effect of 24 h exposure of BALB/3T3 clone A31 cells on unmodified and modified cotton extracts, determined with the NRU test. Viability is shown as a percentage of the negative control (NC; exposure medium treated analogously to the extracts).

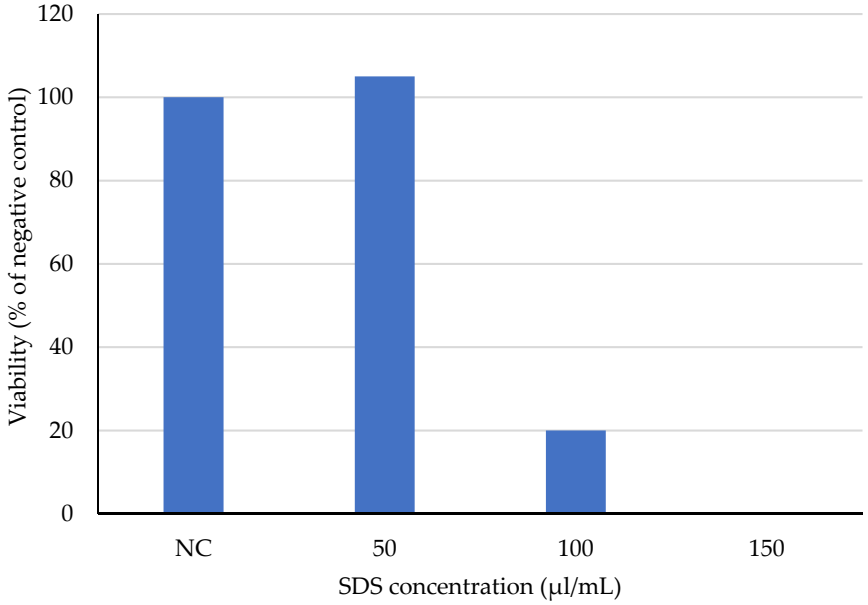

Figure 11. Viability of BALB/3T3 clone A31 cells exposed for 24 h to SDS (positive control), assayed with NRU test. Viability presented as a percentage of the negative control (NC; culture medium with vehicle, i.e., 2% H_2O in culture medium).

Zinc compounds also reveal strong anticancer activity (e.g. [136,179–181]) reflected additionally by nearly 2400 document results on Anticancer Zinc [182] and 1–700 documents results on Anticancer Activity of Zinc abstracted in the Scopus Base [183]. Therefore the COT-Zn composites with cytotoxic activity against BALB/3T3 clone A31 cells should also reveal anticancer character. These investigations will be continued.

4. Conclusions

In summary, COT–Zn composites with different Zn content were prepared by DC magnetron sputtering technology using a zinc metal target. The composite samples were characterized by SEM, EDS, and FAAS. The biological properties of the materials were verified by cytotoxicity screening and antimicrobial activity tests against colonies of *E. coli* and *S. aureus* bacteria and *A. niger* and *C. globosum* fungi. The in vitro determined antimicrobial properties of COT–Zn composites revealed the antibacterial and antifungal activities. In vitro studies showed also that COT–Zn composites containing merely 9 g/kg Zn were cytotoxic. The ability to adapt clean and zero-waste magnetron sputtering methods to an industrial scale provides the possibility to obtain sustainable materials for use in a variety of applications. The prepared fiber composites have great application potential as an antimicrobial material in the field of biomedical engineering (e.g., rehabilitation, medical devices); however, due to their cytotoxicity they have limited possibilities of use as a material interacting with cells of the human body.

Author Contributions: M.H.K. developed the concept and designed experiments, performed the experiments, analyzed the data, and wrote the paper; M.G., P.K. and Z.S. performed the experiments and analyzed the data. All authors have read and agreed to the published version of the manuscript.

Funding: This research was funded by the Polish Ministry of Science and Higher Education within statutory research work carried out at the The Lukasiewicz Research Network -Textile Research Institute, Lodz, Poland.

Institutional Review Board Statement: Not applicable.

Informed Consent Statement: Not applicable.

Data Availability Statement: Not applicable.

Acknowledgments: Dedicated to the memory of Krystyna Pietrucha.

Conflicts of Interest: The authors declare no conflict of interest.

References

1. Scopus Base: 20249 Document Results on Cotton Textiles. Available online: https://www-1scopus-1com-1000014110125.han.p.lodz.pl/results/results.uri?sid=1bbc482d0ac5c58eb43794f6882e404d&src=s&sot=b&sdt=b&origin=searchbasic&rr=&sl=30&s=TITLE-ABS-KEY(cotton%20textiles)&searchterm1=cotton%20textiles&searchTerms=&connectors=&field1=TITLE_ABS_KEY&fields=# (accessed on 3 March 2022).
2. Wilson, J.F.; Toms, S.; Wong, N.D. (Eds.) *The Cotton and Textile Industry: Innovation and Maturity: Case Studies in Industrial History*; Taylor & Francis: London, UK, 2021; pp. 1–99. ISBN 9780429399749.
3. Patterson, G. Cellulose before CELL: Historical themes. *Carbohydr. Polym.* **2021**, *252*, 117182. [CrossRef] [PubMed]
4. Klemm, D.; Heublein, B.; Fink, H.-P.; Bohn, A. Cellulose: Fascinating biopolymer and sustainable raw material. *Angew. Chem. Int. Ed.* **2005**, *44*, 3358–3393. [CrossRef] [PubMed]
5. Klemm, D.; Kramer, F.; Moritz, S.; Lindstrom, T.; Ankerfors, M.; Gray, D.; Dorris, A. Nanocelluloses: A new family of nature-based materials. *Angew. Chem. Int. Ed.* **2011**, *50*, 5438–5466. [CrossRef] [PubMed]
6. Belgacem, M.N.; Gandini, A. (Eds.) *Monomers, Polymers & Composites from Renewable Resources*; Elsevier Science: Amsterdam, The Netherlands, 2008; ISBN 9780080453163.
7. Kolárová, K.; Vosmanská, V.; Rimpelová, S.; Švorcík, V. *Physical-chemical properties of cellulose-based materials and its antibacterial properties in Cellulose and Cellulose Derivatives: Synthesis, Modification and Applications*; Mondal, I.H., Ed.; Nova Science Publisher: Hauppauge, NY, USA, 2015; Chapter 20; pp. 421–454.
8. Singh, S.P.; Soni, B.; Bajpai, S.K. *Chemically Modified Cotton Fibers for Antimicrobial Applications (Book Chapter) in Cellulose-Based Graft Copolymers: Structure and Chemistry*; Thakur, V.K., Ed.; CRC Press Taylor & Francis Group: Boca Raton, FL, USA; London, UK; New York, NY, USA, 2015; pp. 235–270.
9. Rojas, O.J. (Ed.) *Cellulose Chemistry and Properties: Fibers, Nanocelluloses and Advanced Materials*; Springer Int. Pub.: Heidelberg, Switzerland; New York, NY, USA; Dordrecht, Switzerland; London, UK, 2016; Volume 271, ISBN 978-3-319-26015-0.
10. Rol, F.; Belgacem, M.; Gandini, A.; Bras, J. Recent advances in surface-modified cellulose nanofibrils. *Prog. Polym. Sci.* **2019**, *88*, 241–264. [CrossRef]
11. Ageorges, V.; Monteiro, R.; Leroy, S.; Burgess, C.M.; Pizza, M.; Chaucheyras-Durand, F.; Desvaux, M. Molecular determinants of surface colonisation in diarrhoeagenic Escherichia coli (DEC): From bacterial adhesion to biofilm formation. *FEMS Microbiol. Rev.* **2020**, *44*, 314–350. [CrossRef] [PubMed]

12. Granados, A.; Pleixats, R.; Vallribera, A. Recent advances on antimicrobial and anti-inflammatory cotton fabrics containing nanostructures. *Molecules* **2021**, *26*, 3008. [CrossRef]
13. Varshney, S.; Sain, A.; Gupta, D.; Sharma, S. Factors affecting bacterial adhesion on selected textile fibres. *Indian J. Microbiol.* **2021**, *61*, 31–37. [CrossRef]
14. Saidin, S.; Jumat, M.A.; Mohd Amin, N.A.A.; Saleh Al-Hammadi, A.S. Organic and inorganic antibacterial approaches in combating bacterial infection for biomedical application. *Mater. Sci. Eng. C* **2021**, *118*, 111382. [CrossRef]
15. Teixeira, M.A.; Paiva, M.C.; Amorim, M.T.P.; Felgueira, H.P. Electrospun nanocomposites containing cellulose and its derivatives modified with specialized biomolecules for an enhanced wound healing. *Nanomaterials* **2020**, *10*, 557. [CrossRef]
16. Wang, C.-Y.; Makvandi, P.; Zare, E.N.; Tay, F.R.; Niu, L.-N. Advances in antimicrobial organic and inorganic nanocompounds in biomedicine. *Adv. Therap.* **2020**, *3*, 2000024. [CrossRef]
17. El-Alfy, E.A.; El-Bisi, M.K.; Taha, G.M.; Ibrahim, H.M. Preparation of biocompatible chitosan nanoparticles loaded by tetracycline, gentamycin and ciprofloxacin as novel drug delivery system for improvement the antibacterial properties of cellulose based fabrics. *Int. J. Biol. Macromol.* **2020**, *161*, 1247–1260. [CrossRef] [PubMed]
18. Bodor, N.; Kaminski, J.J.; Selk, S. Soft drugs. 1. Labile quaternary ammonium salts as soft antimicrobials. *J. Med. Chem.* **1980**, *23*, 469–474. [CrossRef] [PubMed]
19. Tischer, M.; Pradel, G.; Ohlsen, K.; Holzgrabe, U. Quaternary Ammonium Salts and Their Antimicrobial Potential: Targets or Nonspecific Interactions? *ChemMedChem* **2012**, *7*, 22–31. [CrossRef] [PubMed]
20. Kwaśniewska, D.; Chen, Y.L.; Wieczorek, D. Biological activity of quaternary ammonium salts and their derivatives. *Pathogens* **2020**, *9*, 459. [CrossRef]
21. Yeow, J.; Shanmugam, S.; Corrigan, N.; Kuchel, R.P.; Xu, J.; Boyer, C. A Polymerization-induced self-assembly approach to nanoparticles loaded with singlet oxygen generators. *Macromolecules* **2016**, *49*, 7277–7285. [CrossRef]
22. Blacha-Grzechnik, A. New Approach in the Application of Conjugated Polymers: The Light-Activated Source of Versatile Singlet Oxygen Molecule. *Materials* **2021**, *14*, 1098. [CrossRef]
23. Sun, G.; Worley, S.D. Halamine Chemistry and its Applications in Biocidal Textiles and Polymers. In *Modified Fibers with Medical and Specialty Applications*; Edwards, J.V., Buschle-Diller, G., Goheen, S.C., Eds.; Springer: Dordrecht, The Netherlands, 2006. [CrossRef]
24. Scopus Base: 7.673 Document Results on Antibacterial Zinc. Available online: https://www-1scopus-1com-100001411012f.han.p.lodz.pl/results/results.uri?sid=94895d0abb0adeb79616d9f4561396f8&src=s&sot=b&sdt=b&origin=searchbasic&rr=&sl=34&s=TITLE-ABS-KEY(Antibacterial%20%20Zinc)&searchterm1=Antibacterial%20%20Zinc&searchTerms=&connectors=&field1=TITLE_ABS_KEY&fields= (accessed on 3 March 2022).
25. Vallee, B.L.; Falchuk, K.H. The biochemical basis of zinc physiology. *Physiol. Rev.* **1993**, *73*, 79–118. [CrossRef]
26. Fosmire, G.J. Zinc toxicity. *Am. J. Clin. Nutr.* **1990**, *51*, 225–227. [CrossRef]
27. Cheknev, S.B.; Vostrova, E.I.; Apresova, M.A.; Piskovskaya, L.S.; Vostrov, A.V. Deceleration of bacterial growth in Staphylococcus aureus and Pseudomonas aeruginosa cultures in the presence of copper and zinc cations. *Zh. Mikrobiol. Epidemiol. Immunobiol.* **2015**, *2*, 9–17.
28. Nakashima, T.; Sakagami, Y.; Matsuo, M. Antibacterial efficacy of cotton fabrics chemically modified by metal salts. *Biocontrol Sci.* **2001**, *6*, 9–15. [CrossRef]
29. Ibrahim, N.A.; Gouda, M.; Zairy, W.M. Enhancing easy care and antibacterial functions of cellulose/wool blends. *J. Nat. Fibers* **2008**, *5*, 347–365. [CrossRef]
30. Ibrahim, N.A.; Eid, B.M.; Youssef, M.A.; El-Sayed, S.A.; Salah, A.M. Functionalization of cellulose-containing fabrics by plasma and subsequent metal salt treatments. *Carbohyd. Polym.* **2012**, *90*, 908–914. [CrossRef] [PubMed]
31. Higazy, A.; Hashem, M.; ElShafei, A.; Shaker, N.; Hady, M.A. Development of anti-microbial jute fabrics via in situ formation of cellulose-tannic acid-metal ion complex. *Carbohyd. Polym.* **2010**, *79*, 890–897. [CrossRef]
32. Shankar, S.; Teng, X.; Li, G.; Rhim, J.-W. Preparation, characterization, and antimicrobial activity of gelatin/ZnO nanocomposite films. *Food Hydrocoll.* **2015**, *45*, 264–271. [CrossRef]
33. Shankar, S.; Rhim, J.-W. Effect of Zn salts and hydrolyzing agents on the morphology and antibacterial activity of zinc oxide nanoparticles. *Environ. Chem. Lett.* **2019**, *17*, 1105–1109. [CrossRef]
34. Perelshtein, I.; Perkas, N.; Gedanken, A. Ultrasonic coating of textiles by antibacterial and antibiofilm nanoparticles #31 (Book Chapter). In *Handbook of Ultrasonics and Sonochemistry*; Springer: Singapore, 2016; pp. 967–993.
35. Lotfiman, S.; Ghorbanpour, M. Antimicrobial activity of ZnO/silica gel nanocomposites prepared by a simple and fast solid-state method. *Surf. Coat. Technol.* **2017**, *310*, 129–133. [CrossRef]
36. Pandimurugan, R.; Thambidurai, S. UV protection and antibacterial properties of seaweed capped ZnO nanoparticles coated cotton fabrics. *Int. J. Biol. Macromol.* **2017**, *105*, 788–795. [CrossRef]
37. Wang, S.; Yang, Y.; Lu, A.; Zhang, L. Construction of cellulose/ZnO composite microspheres in NaOH/zinc nitrate aqueous solution via one-step method. *Cellulose* **2019**, *26*, 557–568. [CrossRef]
38. Jones, N.; Ray, B.; Ranjit, K.T.; Manna, A.C. Antibacterial activity of ZnO nanoparticle suspensions on a broad spectrum of microorganisms. *FEMS Microbiol. Lett.* **2008**, *279*, 71–76. [CrossRef]
39. Hoseinnejad, M.; Jafari, S.M.; Katouzian, I. Inorganic and metal nanoparticles and their antimicrobial activity in food packaging applications. *Crit. Rev. Microbiol.* **2018**, *44*, 161–181. [CrossRef]

40. Yuvasravana, R.; George, P.P.; Devanna, N.; Apsana, G. Fabrication and comparison between anti-bacterial properties of metal oxide nanoparticles prepared by a biogenic approach. *J. Bionanosci.* **2018**, *12*, 408–416. [CrossRef]
41. Li, Y.; Liao, C.; Tjong, S.C. Recent advances in zinc oxide nanostructures with antimicrobial activities. *Int. J. Mol. Sci.* **2020**, *21*, 8836. [CrossRef] [PubMed]
42. Geetha, P. Antibacterial and anticancer activities of biogenic synthesized Ag and ZnO NPS. *Int. J. Innov. Technol. Expl. Eng.* **2019**, *8*, 3143–3147. [CrossRef]
43. Hu, H.; Yu, L.; Qian, X.; Chen, Y.; Chen, B.; Li, Y. Chemoreactive nanotherapeutics by metal peroxide based nanomedicine. *Adv. Sci.* **2021**, *8*, 2000494. [CrossRef]
44. Sirelkhatim, A.; Mahmud, S.; Seeni, A.; Kaus, N.H.M.; Ann, L.C.; Bakhori, S.K.M.; Hasan, H.; Mohamad, D. Review on zinc oxide nanoparticles: Antibacterial activity and toxicity mechanism. *Nano-Micro Lett.* **2015**, *7*, 219–242. [CrossRef]
45. Durrant, P.J.; Durrant, B. *Introduction to Advanced Inorganic Chemistry*; Chapter 16. Group IIB element, zinc; Longman, Green &Co., Ltd.: London, UK, 1962; pp. 508–522. ISBN 0582442133/9780582442139.
46. Weibel, D.; Jovanovic, Z.R.; Gálvez, E.; Steinfeld, A. Mechanism of Zn particle oxidation by H_2O and CO_2 in the presence of ZnO. *Chem. Mater.* **2014**, *26*, 6486–6495. [CrossRef]
47. Gunawan, L.; Johari, G.P. Specific heat, melting, crystallization, and oxidation of zinc nanoparticles and their Transmission Electron Microscopy studies. *J. Phys. Chem. C* **2008**, *112*, 20159–20166. [CrossRef]
48. Khanlary, M.R.; Vahedi, V.; Reyhani, A. Synthesis and characterization of ZnO nanowires by thermal oxidation of Zn thin films at various temperatures. *Molecules* **2012**, *17*, 5021–5029. [CrossRef]
49. Cox, J.D.; Wagman, D.D.; Medvedev, V.A. *CODATA Key Values for Thermodynamics*; Hemisphere Publishing Corp.: New York, NY, USA, 1984; Volume 1.
50. Leitner, J.; Kamrádek, M.; Sedmidubský, D. Thermodynamic properties of rock-salt ZnO. *Thermochim. Acta* **2013**, *572*, 1–5. [CrossRef]
51. Li, Y.; Wu, X. The standard molar enthalpies of formation of nano-ZnO particles with different morphologies. *J. Nanomater.* **2015**, *16*, 738909. [CrossRef]
52. Ellmer, K.; Klein, A. ZnO and Its Applications. In *Transparent Conductive Zinc Oxide*; Ellmer, K., Klein, A., Rech, B., Eds.; Springer Series in Materials Science; Springer: Berlin/Heidelberg, Germany, 2008; Volume 104. [CrossRef]
53. Tan, X.-Q.; Liu, J.-Y.; Niu, J.-R.; Liu, J.-Y.; Tian, J.-Y. Recent progress in magnetron sputtering technology used on fabrics. *Materials* **2018**, *11*, 1953. [CrossRef] [PubMed]
54. Li, Y.; Niu, J.; Zhang, W.; Zhang, L.; Shang, E. Influence of aqueous media on the ROS-mediated toxicity of ZnO nanoparticles toward green fluorescent protein-expressing escherichia coli under UV-365 irradiation. *Langmuir* **2014**, *30*, 2852–2862. [CrossRef] [PubMed]
55. Lakshmi Prasanna, V.; Vijayaraghavan, R. Insight into the mechanism of antibacterial activity of ZnO: Surface defects mediated reactive oxygen species even in the dark. *Langmuir* **2015**, *31*, 9155–9162. [CrossRef] [PubMed]
56. Kim, H.R.; Lee, D.; Lee, G.H.; Kim, S.K.; Choi, S.J.; Hwang, E.T.; Maharjan, A.; Kim, B.S.; Kim, D.; Joo, J.H. Origin of Antibacterial Activity of ZnO Nanoparticles: The Roles of Protonic and Electronic Conductions. *Part. Part. Syst. Charact.* **2019**, *36*, 1900141. [CrossRef]
57. Pachaiappan, R.; Rajendran, S.; Show, P.L.; Manavalan, K.; Naushad, M. Metal/metal oxide nanocomposites for bactericidal effect: A review. *Chemosphere* **2021**, *272*, 128607. [CrossRef]
58. Li, M.; Zhu, L.; Lin, D. Toxicity of ZnO nanoparticles to escherichia Coli: Mechanism and the influence of medium components. *Environ. Sci. Technol.* **2011**, *45*, 1977–1983. [CrossRef]
59. Hoseinzadeh, E.; Makhdoumi, P.; Taha, P.; Hossini, H.J.; Makhdoumi, P.; Kamal, M.A.; Ashraf, G. A review on nano-antimicrobials: Metal nanoparticles, methods and mechanisms. *Curr. Drug Metab.* **2017**, *18*, 120–128. [CrossRef]
60. Danilova, T.A.; Danilina, G.A.; Adzhieva, A.A.; Vostrova, E.I.; Zhukhovitskii, V.G.; Cheknev, S.B. Inhibitory effect of copper and zinc ions on the growth of Streptococcus pyogenes and Escherichia coli Biofilms. *Bull. Exp. Biol. Med.* **2020**, *169*, 648–652. [CrossRef]
61. Sapkota, A.; Anceno, A.J.; Baruah, S.; Shipin, O.V.; Dutta, J. Zinc oxide nanorod mediated visible light photoinactivation of model microbes in water. *Nanotechnology* **2011**, *22*, 215703. [CrossRef]
62. Vigneshwaran, N.; Kumar, S.; Kathe, A.A.; Varadarajan, P.V.; Prasad, V. Functional finishing of cotton fabrics using zinc oxide-soluble starch nanocomposites. *Nanotechnology* **2006**, *17*, 5087–5095. [CrossRef]
63. Perelshtein, I.; Applerot, G.; Perkas, N.; Wehrschetz-Sigl, E.; Hasmann, A.; Guebitz, G.M.; Gedanken, A. Antibacterial properties of an in situ generated and simultaneously deposited nanocrystalline ZnO on fabrics. *ACS Appl. Mater. Interfaces* **2009**, *1*, 361–366. [CrossRef] [PubMed]
64. Petkova, P.; Francesko, A.; Fernandes, M.M.; Mendoza, E.; Ilana Perelshtein, I.; Gedanken, A.; Tzanov, T. Sonochemical coating of textiles with hybrid ZnO/chitosan antimicrobial nanoparticles. *ACS Appl. Mater. Interfaces* **2014**, *6*, 1164–1172. [CrossRef] [PubMed]
65. Petkova, P.; Francesko, A.; Perelshtein, I.; Gedanken, A.; Tzanov, T. Simultaneous sonochemical-enzymatic coating of medical textiles with antibacterial ZnO nanoparticles. *Ultrason. Sonochem.* **2016**, *29*, 244–250. [CrossRef] [PubMed]
66. Hu, R.; Yang, J.; Yang, P.; Wu, Z.; Xiao, H.; Liu, Y.; Lu, M. Fabrication of ZnO@Cotton fabric with anti-bacterial and radiation barrier properties using an economical and environmentally friendly method. *Cellulose* **2020**, *27*, 2901–2911. [CrossRef]
67. Selvam, S.; Sundrarajan, M. Functionalization of cotton fabric with PVP/ZnO nanoparticles for improved reactive dyeability and antibacterial activity. *Carbohydr. Polym.* **2012**, *87*, 1419–1424. [CrossRef]
68. Ugur, S.S.; Sariisik, M.; Aktas, A.H.; Ucar, M.C.; Erden, E. Modifying of cotton fabric surface with Nano-ZnO multilayer films by Layer-by-Layer deposition method. *Nanoscale Res. Lett.* **2010**, *5*, 1204–1210. [CrossRef]

69. El-Naggar, M.E.; Hassabo, A.G.; Mohamed, A.L.; Shaheen, T.I. Surface modification of SiO_2 coated ZnO nanoparticles for multifunctional cotton fabrics. *J. Colloid Interf. Sci.* **2017**, *498*, 413–422. [CrossRef]
70. Shaheen, T.; El-Naggar, M.E.; Abdelgawad, A.M.; Hebeish, A. Durable antibacterial and UV protections of in situ synthesized zinc oxide nanoparticles onto cotton fabrics. *Int. J. Biol. Macromol.* **2016**, *83*, 426–432. [CrossRef]
71. Shaban, M.; Mohamed, F.; Abdallah, S. Production and characterization of superhydrophobic and antibacterial coated fabrics utilizing ZnO nanocatalyst. *Sci. Rep.* **2018**, *8*, 3925. [CrossRef]
72. Shateri-Khalilabad, M.; Yazdanshenas, M.E. Bifunctionalization of cotton textiles by ZnO nanostructures: Antimicrobial activity and ultraviolet protection. *Text. Res. J.* **2013**, *83*, 993–1004. [CrossRef]
73. Fouda, A.; EL-Din Hassan, S.; Salem, S.S.; Shaheen, T.I. In-Vitro cytotoxicity, antibacterial, and UV protection properties of the biosynthesized Zinc oxide nanoparticles for medical textile applications. *Microb. Pathog.* **2018**, *125*, 252–261. [CrossRef] [PubMed]
74. Musil, J.; Vlcek, J. Magnetron sputtering of films with controlled texture and grain size. *Mater. Chem. Phys.* **1998**, *54*, 116–122. [CrossRef]
75. Kelly, P.; Arnell, R.D. Magnetron Sputtering: A Review of Recent Developments and Applications. *Vacuum* **2000**, *56*, 159–172. [CrossRef]
76. Dinescu, G.; Ruset, C.; Dinescu, M. Trends in combining techniques for the deposition of new application-tailored thin films. *Plasma Process. Polym.* **2007**, *4*, 282–292. [CrossRef]
77. Shahidi, S.; Ghoranneviss, M.; Moazzenchi, B.; Rashidi, A.; Mirjalili, M. Investigation of antibacterial activity on cotton fabrics with cold plasma in the presence of a magnetic field. *Plasma Process. Polym.* **2007**, *4*, 1098–1103. [CrossRef]
78. Han, J.G. Recent progress in thin film processing by magnetron sputtering with plasma diagnostics. *J. Phys. D Appl. Phys.* **2009**, *42*, 043001. [CrossRef]
79. Gorberg, B.L.; Ivanov, A.A.; Mamontov, O.V.; Stegnin, V.A.; Titov, V.A. Modification of textile materials by the deposition of nanocoatings by magnetron ion-plasma sputtering. *Russ. J. Gen. Chem.* **2013**, *83*, 157–163. [CrossRef]
80. Zhang, H.; Cherng, J.-S.; Chen, Q. Recent progress on high power impulse magnetron sputtering (HiPIMS): The challenges and applications in fabricating VO2 thin film. *AIP Adv.* **2019**, *9*, 035242. [CrossRef]
81. Scopus Base: 11805 Document Results on Zinc Sputtering. Available online: https://www-1scopus-1com-10000141101be.han.p.lodz.pl/results/results.uri?sid=45b2d096db1d5d687abc015e8271c5b8&src=s&sot=b&sdt=b&origin=searchbasic&rr=&sl=30&s=TITLE-ABS-KEY(zinc%20sputtering)&searchterm1=zinc%20sputteringsearchTerms=&connectors=&field1=TITLE_ABS_KEY&fields= (accessed on 3 March 2022).
82. Scopus Base: 289 Document Results on Polymer Zinc Sputtering. Available online: https://www-1scopus-1com-10000141101be.han.p.lodz.pl/results/results.uri?sid=d4411dea1a4b0222c939239a6a49e873&src=s&sot=b&sdt=b&origin=searchbasic&rr=&sl=38&s=TITLE-ABS-KEY(polymer%20zinc%20sputtering)&searchterm1=polymer%20zinc%20sputtering&searchTerms=&connectors=&field1=TITLE_ABS_KEY&fields= (accessed on 3 March 2022).
83. Bachari, E.M.; Ben Amor, S.; Baud, G.; Jacquet, M. Photoprotective zinc oxide coatings on polyethylene terephthalate films. *Mater. Sci. Eng. B Solid State Mater. Adv. Technol.* **2001**, *79*, 165–174. [CrossRef]
84. Koidis, C.; Logothetidis, S.; Georgiou, D.; Laskarakis, A.; Lousinian, S.; Tsiaoussis, I.; Frangis, N. Growth, optical and nanostructural properties of magnetron sputtered ZnO thin films deposited on polymeric substrates. *Phys. Status Solidi A* **2008**, *205*, 1988–1992. [CrossRef]
85. Amor, S.B.; Jacquet, M.; Fioux, P.; Nardin, M. XPS characterisation of plasma treated and zinc oxide coated PET. *Appl. Surf. Sci.* **2009**, *255*, 5052–5061. [CrossRef]
86. Garganourakis, M.; Logothetidis, S.; Pitsalidis, C.; Georgiou, D.; Kassavetis, S.; Laskarakis, A. Deposition and characterization of PEDOT/ZnO layers onto PET substrates. *Thin Solid Films* **2009**, *517*, 6409–6413. [CrossRef]
87. Ben Amor, S.; Jacquet, M.; Fioux, P.; Nardin, M. A ZnO/PET assembly study: Optimization and investigation of the interface region. *Mater. Chem. Phys.* **2010**, *119*, 158–168. [CrossRef]
88. Sierros, K.A.; Banerjee, D.A.; Morris, N.J.; Cairns, D.R.; Kortidis, I.; Kiriakidis, G. Mechanical properties of ZnO thin films deposited on polyester substrates used in flexible device applications. *Thin Solid Films* **2010**, *519*, 325–330. [CrossRef]
89. Fahlteich, J.; Schönberger, W.; Fahland, M.; Schiller, N. Characterization of reactively sputtered permeation barrier materials on polymer substrates. *Surf. Coat. Technol.* **2011**, *205* (Suppl. 2), S141–S144. [CrossRef]
90. Wang, S.S.; Yang, C.B.; Shiou, F.J.; Hsu, C.Y. Structural properties of Ga-doped ZnO films grown on polymer substrates. *J. Comp. Theoret. Nanosci.* **2014**, *11*, 751–756. [CrossRef]
91. Imran, M.; Ahmad, R.; Afzal, N.; Rafique, M. Copper ion implantation effects in ZnO film deposited on flexible polymer by DC magnetron sputtering. *Vacuum* **2019**, *165*, 72–80. [CrossRef]
92. Guedri-Knani, L.; Gardette, J.L.; Jacquet, M.; Rivaton, A. Photoprotection of poly(ethylene-naphthalate) by zinc oxide coating. *Surf. Coat. Technol.* **2004**, *180–181*, 71–75. [CrossRef]
93. Guedri, L.; Ben Amor, S.; Gardette, J.L.; Jacquet, M.; Rivaton, A. Lifetime improvement of poly(ethylene naphthalate) by ZnO adhesive coatings. *Polym. Degrad. Stab.* **2005**, *88*, 199–205. [CrossRef]
94. Liu, Y.-Y.; Yuan, Y.-Z.; Gao, X.-T.; Yan, S.; Cao, X.-Z.; Wei, G.-X. Deposition of ZnO thin film on polytetrafluoroethylene substrate by the magnetron sputtering method. *Mater. Lett.* **2007**, *61*, 4463–4465. [CrossRef]
95. Liu, Y.-Y.; Yuan, Y.-Z.; Li, C.-F.; Gao, X.; Cao, X.-Z.; Li, J.-B. The structure and photoluminescence properties of RF-sputtered films of ZnO on Teflon substrate. *Mater. Lett.* **2008**, *62*, 2907–2909. [CrossRef]
96. Liu, Y.-Y.; Zang, Y.-L.; Wei, G.-X.; Li, J.; Fan, X.-L.; Cheng, C.-F. Stress and structural studies of ZnO thin films on polymer substrate under different RF powered conditions. *Mater. Lett.* **2009**, *63*, 2597–2599. [CrossRef]

97. Liu, Y.; Wang, R.; Wei, G.; Cui, D.; Wang, H. Effect of deposition pressure on the properties of zno films on teflon substrate by RF magnetron sputtering. *Acta Microsc.* **2019**, *28*, 391–396.
98. Pál, E.; Seemann, T.; Zöllmer, V.; Busse, M.; Dékány, I. Hybrid ZnO/polymer thin films prepared by RF magnetron sputtering. *Colloid Polym. Sci.* **2009**, *287*, 481–485. [CrossRef]
99. Wei, Q.; Yu, L.; Hou, D.; Huang, F. Surface characterization and properties of functionalized nonwoven. *J. Appl. Polym. Sci.* **2008**, *107*, 132–137. [CrossRef]
100. Singh, A.; Schipmann, S.; Mathur, A.; Pal, D.; Sengupta, A.; Klemradt, U.; Chattopadhyay, S. Structure and morphology of magnetron sputter deposited ultrathin ZnO films on confined polymeric template. *Appl. Surf. Sci.* **2019**, *414*, 114–123. [CrossRef]
101. Giancaterina, S.; Ben Amor, S.; Baud, G.; Gardette, J.L.; Jacquet, M.; Perrin, C.; Rivaton, A. Photoprotective ceramic coatings on poly(ether ether ketone). *Polymer* **2002**, *43*, 6397–6405. [CrossRef]
102. Yoo, D.; Choi, M.-S.; Chung, C.; Heo, S.C.; Kim, D.; Choi, C. Characteristics of radio frequency-sputtered ZnS on the flexible polyethylene terephthalate (PET) substrate. *J. Nanosci. Nanotechnol.* **2013**, *13*, 7814–7819. [CrossRef]
103. Fortunato, E.; Godinho, M.H.; Santos, H.; Marques, A.; Assunção, V.; Pereira, L.; Águas, H.; Ferreira, I.; Martins, R. Surface modification of a new flexible substrate based on hydroxypropylcellulose for optoelectronic applications. *Thin Solid Films* **2003**, *442*, 127–131. [CrossRef]
104. Wei, Q.; Xu, Q.; Cai, Y.; Gao, W.; Bo, C. Characterization of polymer nanofibers coated by reactive sputtering of zinc. *J. Mater. Process. Technol.* **2009**, *209*, 2028–2032. [CrossRef]
105. Pertsin, A.I.; Volkov, I.O. Interaction of zinc atoms with polymer surfaces. *Vysokomol. Soed. Ser. A* **1996**, *38*, 1249–1253.
106. Kudzin, M.H.; Mrozinska, Z.; Urbaniak, P. Vapor phosphorylation of cellulose by phosphorus trichloride: Selective phosphorylation of 6-hydroxyl function—The synthesis of new antimicrobial Cellulose 6-Phosphate(III)-Copper complexes. *Antibiotics* **2021**, *10*, 203. [CrossRef] [PubMed]
107. Kudzin, M.H.; Mrozińska, Z.; Łatwińska, M.; Urbaniak, P.; Drabowicz, J. Stability of cellulose phosphates in alkalic solutions. *Phosphorus Sulfur Silicon Relat. Elem.* **2022**. [CrossRef]
108. Kudzin, M.H.; Mrozińska, Z.; Urbaniak, P.; Drabowicz, J. Surface phosphorylation of cellulose by means of PCl_3 and $P(O)Cl_3$. *Phosphorus Sulfur Silicon Relat. Elem.* **2021**. [CrossRef]
109. Kudzin, M.H.; Giełdowska, M.; Krata, A.A.; Sulak, E.; Urbaniak, P.; Drabowicz, J. Surface phosphorylation of chitosan by means of PCl_3. *Phosphorus Sulfur Silicon Relat. Elem.* **2021**. [CrossRef]
110. Kudzin, M.H.; Mrozinska, Z. Biofunctionalization of textile materials. 3. Biofunctionalization of poly(lactide) (PLA) nonwovens fabrics by KI. *Coatings* **2020**, *10*, 593. [CrossRef]
111. Kudzin, M.H.; Mrozinska, Z.; Walawska, A.; Sójka-Ledakowicz, J. Biofunctionalization of textile materials.1. Biofunctionalization of poly(propylene) (PP) nonwovens fabrics by Alafosfalin. *Coatings* **2019**, *9*, 412. [CrossRef]
112. Kudzin, M.H.; Mrozinska, Z. Biofunctionalization of textile materials. 2. Antimicrobial modification of poly(lactide) (PLA) nonwoven fabrics by fosfomycin. *Polymers* **2020**, *12*, 768. [CrossRef]
113. Kudzin, M.H.; Kudzin, Z.H.; Drabowicz, J. Thioureidoalkylphosphonates in the synthesis of 1-aminoalkylphosphonic acids. The Ptc-aminophosphonate method. *Arkivoc* **2011**, *6*, 227–269. [CrossRef]
114. Drabowicz, J.; Jakubowski, H.; Kudzin, M.H.; Kudzin, Z.H. The nomenclature of 1-aminoalkylphosphonic acids and derivatives: Evolution of the code system. *Acta Biochim. Pol.* **2015**, *62*, 139–150. [CrossRef]
115. *Analytical Methods for Atomic Absorption Spectroscopy*; The Perkin-Elmer Corporation: Waltham, MA, USA, 1996; Volume 46, Available online: www.perkinelmer.com (accessed on 3 July 2020).
116. *EN ISO 20645:2006*; Textile Fabrics. Determination of Antibacterial Activity—Agar Diffusion Plate Test. International Organization for Standardization: Geneva, Switzerland, 2006.
117. *EN 14119:2005*; Testing of Textiles. Evaluation of the Action of Microfungi. Visual Method. International Organization for Standardization: Geneva, Switzerland, 2005.
118. *EN 1ISO 10993-12:2012*; Biological evaluation of medical devices—Part 12: Sample preparation and reference materials. International Organization for Standardization: Geneva, Switzerland, 2012.
119. Panchakarla, L.S.; Govindaraj, A.; Rao, C.N.R. Formation of ZnO nanoparticles by the reaction of zinc metal with aliphatic alcohols. *J. Clust. Sci.* **2007**, *18*, 660–670. [CrossRef]
120. Shah, M.A. Formation of zinc oxide nanoparticles by the reaction of zinc metal with methanol at very low temperature. *Afr. Phys. Rev.* **2008**, *2*, 106–109.
121. Shah, M.A. Growth of zinc oxide nanoparticles by the reaction of zinc with ethanol. In *Advanced Materials Research*; Trans Tech Publications, Ltd.: Freienbach, Switzerland, 2009; Volume 67, pp. 215–219. [CrossRef]
122. Shah, M.A. Synthesis of zinc oxide nanoparticles by the reaction of zinc metal with ethanol. *Mod. Phys. Lett. B* **2009**, *23*, 871–876. [CrossRef]
123. Ekem, N.; Korkmaz, S.; Pat, S.; Balbag, M.Z.; Cetin, E.N.; Ozmumcu, M. Some physical properties of ZnO thin films prepared by RF sputtering technique. *Int. J. Hydrog. Energy* **2009**, *34*, 5218–5222. [CrossRef]
124. Fenske, F.; Fuhs, W.; Nebauer, E.; Schopke, A.; Selle, B.; Sieber, I. Transparent conductive ZnO:Al films by reactive co-sputtering from separate metallic Zn and Al targets. *Thin Solid Films* **1999**, *343–344*, 130–133. [CrossRef]
125. Wasim, M.; Khan, M.R.; Mushtaq, M.; Neem, A.; Han, M.; Wei, Q. Surface modification of bacterial cellulose by copper and Zinc Oxide sputter coating for UV-resistance/antistatic/antibacterial characteristics. *Coatings* **2020**, *10*, 364. [CrossRef]

126. Chao, L.-C.; Lin, C.-F.; Liau, C.-C. Effect of surface morphology of metallic zinc films deposited by ion beam sputter deposition on the formation of ZnO nanowires. *Vacuum* **2011**, *86*, 295–298. [CrossRef]
127. Abdalkader, D.; Al-Saedi, F. Antibacterial Effect of Different Concentrations of Zinc Sulfate on Multidrug Resistant Pathogenic Bacteria. *Syst. Rev. Pharm.* **2020**, *11*, 282–288. [CrossRef]
128. Jayandran, M.; Haneefa, M.M.; Balasubramanian, V. Synthesis, characterization and antimicrobial activities of turmeric curcumin and curcumin stabilized zinc nanoparticles—A green approach. *Res. J. Pharm. Technol.* **2015**, *8*, 445–451. [CrossRef]
129. Khan, F.A.; Khan, Z.U.H.; Ma, J.; Khan, A.U.; Sohail, M.; Chen, Y.; Yang, Y.; Pan, X. An Astragalus membranaceus based eco-friendly biomimetic synthesis approach of ZnO nanoflowers with an excellent antibacterial, antioxidant and electrochemical sensing effect. *Mater. Sci. Eng.* **2021**, *118*, 111432. [CrossRef]
130. Haghgoo, R.; Ahmadvand, M.; Nyakan, M.; Jafari, M. Antimicrobial efficacy of mixtures of nanosilver and zinc oxide eugenol against Enterococcus faecalis. *J. Contemp. Dent. Pract.* **2017**, *18*, 177–181. [CrossRef] [PubMed]
131. Abu Ali, H.; Omar, S.N.; Darawsheh, M.D.; Fares, H. Synthesis, characterization and antimicrobial activity of zinc(II) ibuprofen complexes with nitrogen-based ligands. Synthesis, characterization and antimicrobial activity of zinc(II) ibuprofen complexes with nitrogen-based ligands. *J. Coord. Chem.* **2016**, *69*, 1110–1122. [CrossRef]
132. Danial, E.N.; Yousef, J.M. Comparative studies between zinc oxide and manganese oxide nano-particle for their antimicrobial activities. *J. Pure Appl. Microbiol.* **2014**, *8*, 293–300.
133. Senthilraja, A.; Krishnakumar, B.; Hariharan, R.; Sobral, A.J.F.N.; Surya, C.; John, N.A.A.; Shanthi, M. Synthesis and characterization of bimetallic nanocomposite and its photocatalytic, antifungal and antibacterial activity. *Sep. Purif. Technol.* **2018**, *202*, 373–384. [CrossRef]
134. Negi, A.; Gangwar, R.; Vishwakarma, R.K.; Negi, D.S. Biogenic zinc oxide nanoparticles as an antibacterial, antifungal, and photocatalytic tool mediated via leaves of Girardinia diversifolia. *Nanotechnol. Environ. Eng.* **2022**, *7*, 223–233. [CrossRef]
135. Mekky, A.E.; Farrag, A.A.; Hmed, A.A.; Sofy, A.R. Preparation of zinc oxide nanoparticles using aspergillus niger as antimicrobial and anticancer agents. *J. Pure Appl. Microbiol.* **2021**, *15*, 1547–1566. [CrossRef]
136. Vidhya, E.; Vijayakumar, S.; Prathipkumar, S.; Praseetha, P.K. Green way biosynthesis: Characterization, antimicrobial and anticancer activity of ZnO nanoparticles. *Gene Rep.* **2020**, *20*, 100688. [CrossRef]
137. Umavathi, S.; Ramya, M.; Padmapriya, C.; Gopinath, K. Green Synthesis of Zinc Oxide Nanoparticle Using Justicia procumbense Leaf Extract and Their Application as an Antimicrobial Agent. *J. Biol. Act. Prod. Nat.* **2020**, *10*, 153–164. [CrossRef]
138. Muthuchamy, M.; Muneeswaran, T.; Rajivgandhi, G.; Christophe Quero, F.; Muthusamy, A.; Ji-Ming, S. Biologically synthesized copper and zinc oxide nanoparticles for important biomolecules detection and antimicrobial applications. *Mater. Today Commun.* **2020**, *22*, 100766. [CrossRef]
139. Pillai, A.M.; Sivasankarapillai, V.S.; Rahdar, A.; Joseph, J.; Sadeghfar, F.; Anuf, R.; Rajesh, K.; Kyzas, G.Z. Green synthesis and characterization of zinc oxide nanoparticles with antibacterial and antifungal activity. *J. Mol. Struct.* **2020**, *1211*, 128107. [CrossRef]
140. Sandhya, J.; Kalaiselvam, S. UV responsive quercetin derived and functionalized CuO/ZnO nanocomposite in ameliorating photocatalytic degradation of rhodamine B dye and enhanced biocidal activity against selected pathogenic strains. *J. Environ. Sci. Health-Toxic/Hazard.* **2021**, *56*, 835–848. [CrossRef] [PubMed]
141. Alioui, H.; Bouras, O.; Bollinger, J.-C. Toward an efficient antibacterial agent: Zn- and Mg-doped hydroxyapatite nanopowders. *J. Environ. Sci. Health-Toxic/Hazard.* **2019**, *54*, 315–327. [CrossRef] [PubMed]
142. Sun, X.; Yin, L.; Zhu, H.; Zhu, J.; Hu, J.; Luo, X.; Huang, H.; Fu, Y. Enhanced Antimicrobial Cellulose/Chitosan/ZnO Biodegradable Composite Membrane. *Membranes* **2022**, *12*, 239. [CrossRef] [PubMed]
143. Suryanegar, L.; Fatriasari, W.; Zulfiana, D.; Anita, S.H.; Masruchin, N.; Gutari, S.; Kemala, T. Novel antimicrobial bioplastic based on PLA-chitosan by addition of TiO_2 and ZnO. *J. Environ. Health Sci. Eng.* **2021**, *19*, 415–425. [CrossRef]
144. Ibrahim, S.; El-Naggar, M.E.; Youssef, A.M.; Abdel-Aziz, M.S. Functionalization of polystyrene nanocomposite with excellent antimicrobial efficiency for food packaging application. *J. Clust. Sci.* **2020**, *31*, 1371–1382. [CrossRef]
145. Odell, E.; Pertl, C. Zinc as a growth factor for Aspergillus sp. and the antifungal effects of root canal sealants. *Oral Surg. Oral Med. Oral Pathol. Oral Radiol. Endod.* **1995**, *79*, 82–87. [CrossRef]
146. Kudzin, M.H.; Giełdowska, M.; Mrozinska, Z.; Bogun, M. Poly(lactic acid)/Zinc/Alginate Complex Material: Preparation and Antimicrobial Properties. *Antibiotics* **2021**, *10*, 1327. [CrossRef]
147. Lam, S.-M.; Lim, C.-L.; Sin, J.-C.; Zeng, H.; Lin, H.; Li, H. Facile synthesis of MnO_2/ZnO coated on cotton fabric for boosted antimicrobial, self-cleaning and photocatalytic activities under sunlight. *Mater. Lett.* **2021**, *305*, 130818. [CrossRef]
148. Siddiqi, K.S.; ur Rahman, A.; Tajuddin; Husen, A. Properties of zinc oxide nanoparticles and their activity against microbes. *Nanoscale Res. Lett.* **2018**, *13*, 141. [CrossRef]
149. Takahashi, H.; Koshi, K. Solubility and cell toxicity of cobalt, zinc and lead. *Ind. Health* **1981**, *19*, 47–59. [CrossRef]
150. David, C.A.; Galceran, J.; Rey-Castro, C.; Puy, J.; Companys, E.; Salvador, J.; Monné, J.; Wallace, R.; Vakourov, A. Dissolution kinetics and solubility of ZnO nanoparticles followed by AGNES. *J. Phys. Chem. C* **2012**, *116*, 11758–11767. [CrossRef]
151. Wu, F.; Harper, B.J.; Harper, S.L. Comparative dissolution, uptake, and toxicity of zinc oxide particles in individual aquatic species and mixed populations. *Environ. Toxicol. Chem.* **2019**, *38*, 591–602. [CrossRef] [PubMed]
152. Cao, D.; Gong, S.; Shu, X.; Zhu, D.; Liang, S. Preparation of ZnO nanoparticles with high dispersibility based on oriented attachment (OA) process. *Nanoscale Res. Lett.* **2019**, *14*, 210. [CrossRef] [PubMed]

153. Lee, W.; Yeop, J.; Heo, J.; Yoon, Y.J.; Park, S.Y.; Jeong, J.; Shin, Y.S.; Kim, J.W.; An, N.G.; Kim, D.S.; et al. High colloidal stability ZnO nanoparticles independent on solvent polarity and their application in polymer solar cells. *Sci. Rep.* **2020**, *10*, 18055. [CrossRef]
154. Stoddart, M. (Ed.) *Mammalian Cell Viability. Methods in Molecular Biology (Methods and Protocols)*; Humana Press: New York, NY, USA; Springer: Dordrecht, The Netherlands; Heidelberg, Germany; London, UK, 2011; Volume 740. [CrossRef]
155. Riss, T.L.; Moravec, R.A.; Niles, A.L.; Duellman, S.; Benink, H.A.; Worzella, T.J.; Minor, L. Cell Viability Assays. In *Assay Guidance Manual*; Markossian, S., Grossman, A., Brimacombe, K., Arkin, M., Auld, D., Austin, C.P., Baell, J., Chung, T.D.Y., Coussens, N.P., Dahlin, J.L., et al., Eds.; Eli Lilly & Company and the National Center for Advancing Translational Sciences: Bethesda, MD, USA, 2016.
156. Garcia-Hernando, M.; Benito-Lopez, F.; Basabe-Desmonts, L. Advances in Microtechnology for Improved Cytotoxicity Assessment. *Front. Mater.* **2020**, *7*, 582030. [CrossRef]
157. Chiellini, F. Perspectives on: In vitro evaluation of biomedical polymers. *J. Bioact. Compat. Polym.* **2006**, *21*, 257–271. [CrossRef]
158. Goldberg, M.; Langer, R.; Jia, X. Nanostructured materials for applications in drug delivery and tissue engineering. *J. Biomater. Sci. Polym. Ed.* **2007**, *18*, 241–268. [CrossRef]
159. Hu, J.; Tang, Y.; Elmenoufy, A.H.; Xu, H.; Cheng, Z.; Yang, X. Nanocomposite-based photodynamic therapy strategies for deep tumor treatment. *Small* **2015**, *11*, 5860–5887. [CrossRef]
160. Naskar, A.; Kim, K.-S. Recent advances in nanomaterial-based wound-healing therapeutics. *Pharmaceutics* **2020**, *12*, 499. [CrossRef]
161. Yetisgin, A.A.; Cetinel, S.; Zuvin, M.; Kosar, A.; Kutlu, O. Therapeutic nanoparticles and their targeted delivery applications. *Molecules* **2020**, *25*, 2193. [CrossRef]
162. Ali, E.S.; Sharker, S.M.; Islam, M.T.; Khan, I.N.; Shaw, S.; Rahman, A.; Uddin, S.J.; Shill, M.C.; Rehman, S.; Das, N.; et al. Targeting cancer cells with nanotherapeutics and nanodiagnostics: Current status and future perspectives. *Cancer Biol.* **2021**, *69*, 52–68. [CrossRef] [PubMed]
163. Nikzamir, M.; Akbarzadeh, A.; Panahi, Y. An overview on nanoparticles used in biomedicine and their cytotoxicity. *J. Drug Deliv. Sci. Technol.* **2021**, *61*, 102316. [CrossRef]
164. Sharma, S.; Sudhakara, P.; Singh, J.; Ilyas, R.A.; Asyraf, M.R.M.; Razman, M.R. Critical review of biodegradable and bioactive polymer composites for bone tissue engineering and drug delivery applications. *Polymers* **2021**, *13*, 2623. [CrossRef] [PubMed]
165. Repetto, G.; del Peso, A.; Zurita, J.L. Neutral red uptake assay for the estimation of cell viability/cytotoxicity. *Nat. Protoc.* **2008**, *3*, 1125–1131. [CrossRef] [PubMed]
166. Liao, C.; Jin, Y.; Li, Y.; Tjong, S.C. Interactions of zinc oxide nanostructures with mammalian cells: Cytotoxicity and photocatalytic toxicity. *Int. J. Mol. Sci.* **2020**, *21*, 6305. [CrossRef] [PubMed]
167. Yang, H.; Liu, C.; Yang, D.; Zhang, H.; Xi, Z. Comparative study of cytotoxicity, oxidative stress and genotoxicity induced by four typical nanomaterials: The role of particle size, shape and composition. *J. Appl. Toxicol.* **2009**, *29*, 69–78. [CrossRef]
168. Heng, B.C.; Zhao, X.; Xiong, S.; Ng, K.W.; Boey, F.Y.-C.; Loo, J.S.-C. Cytotoxicity of zinc oxide (ZnO) nanoparticles is influenced by cell density and culture format. *Archiv. Toxicol.* **2011**, *85*, 695–704. [CrossRef]
169. Saptarshi, S.R.; Duschl, A.; Lopata, A.L. Biological reactivity of zinc oxide nanoparticles with mammalian test systems: An overview. *Nanomedicine* **2015**, *10*, 2075–2092. [CrossRef]
170. Bisht, G.; Rayamajhi, S. ZnO Nanoparticles: A promising anticancer agent. *Nanobiomedicine* **2016**, *3*, 9. [CrossRef]
171. Scherzad, A.; Meyer, T.; Kleinsasser, N.; Hackenberg, S. Molecular mechanisms of Zinc oxide Nanoparticle-induced genotoxicity short running title: Genotoxicity of ZnO NPs. *Materials* **2017**, *10*, 1427. [CrossRef]
172. Cordani, M.; Somoza, Á. Targeting autophagy using metallic nanoparticles: A promising strategy for cancer treatment. *Cell. Mol. Life Sci.* **2019**, *76*, 1215–1242. [CrossRef] [PubMed]
173. Czyżowska, A.; Barbasz, A. Cytotoxicity of zinc oxide nanoparticles to innate and adaptive human immune cells. *J. Appl. Toxicol.* **2021**, *41*, 1425–1437. [CrossRef] [PubMed]
174. Mukherjee, S.; Shil, A.; Pal, K.; Pal, S.; Sikdar, M. Comparative evaluation of the antibacterial and cytotoxic activity of green synthesized and commercially available ZnO nanoparticles. *Biomedicine* **2021**, *41*, 565–575. [CrossRef]
175. Alkhudhayri, A.A. A comparative cytotoxic study against breast cancer cells with nanoparticles and rods shaped structures. *J. King Saud Univ. Sci.* **2022**, *34*, 101797. [CrossRef]
176. Gong, Y.; Ji, Y.; Liu, F.; Li, J.; Cao, Y. Cytotoxicity, oxidative stress and inflammation induced by ZnO nanoparticles in endothelial cells: Interaction with palmitate or lipopolysaccharide. *J. Appl. Toxicol.* **2017**, *37*, 895–901. [CrossRef] [PubMed]
177. Yan, D.; Long, J.; Liu, J.; Cao, Y. The toxicity of ZnO nanomaterials to HepG2 cells: The influence of size and shape of particles. *J. Appl. Toxicol.* **2019**, *39*, 231–240. [CrossRef]
178. Liebsch, H.M.; Spielmann, H. Balb/c 3T3 cytotoxicity test. *Methods Mol. Biol.* **1995**, *43*, 177–187. [CrossRef]
179. Rasmussen, J.W.; Martinez, E.; Louka, P.; Wingett, D.G. Zinc oxide nanoparticles for selective destruction of tumor cells and potential for drug delivery applications. *Expert Opin. Drug Deliv.* **2010**, *7*, 1063–1077. [CrossRef]
180. Vakayil, R.; Muruganantham, S.; Kabeerdass, N.; Rajendran, M.; Mahadeopalve, A.; Ramasamy, S.; Alahmadi, T.A.; Almoallim, H.S.; Manikandan, V.; Mathanmohun, M. Acorus calamus-zinc oxide nanoparticle coated cotton fabrics shows antimicrobial and cytotoxic activities against skin cancer cells. *Process Biochem.* **2021**, *111*, 1–8. [CrossRef]
181. Zhang, Y.; Guo, C.; Liu, L.; Xu, J.; Jiang, H.; Li, D.; Lan, J.; Li, J.; Yang, J.; Tu, Q.; et al. ZnO-based multifunctional nanocomposites to inhibit progression and metastasis of melanoma by eliciting antitumor immunity via immunogenic cell death. *Theranostics* **2020**, *10*, 11197–11214. [CrossRef]

182. Scopus Base: 2 385 document results on Anticancer Zinc. Available online: https://www-1scopus-1com-1000014xv00bf.han.p.lodz.pl/results/results.uri?sort=plf-f&src=s&st1=anticancer+++zinc&sid=99008ee26e21b10041dcc27109299b0d&sot=b&sdt=b&sl=32&s=TITLE-ABS-KEY%28anticancer+++zinc%29&origin=searchbasic&editSaveSearch=&yearFrom=Before+1960&yearTo=Present (accessed on 3 March 2022).
183. Scopus Base: 1695 document results on Anticancer Activity of Zinc. Available online: https://www-1scopus-1com-1000014rj027e.han.p.lodz.pl/results/results.uri?sort=plf-f&src=s&st1=anticancer+activity+of+zinc&sid=346666e547acd8834d6266afbda418b8&sot=b&sdt=b&sl=42&s=TITLE-ABS-KEY%28anticancer+activity+of+zinc%29&origin=searchbasic&editSaveSearch=&yearFrom=Before+1960&yearTo=Present (accessed on 3 March 2022).